# Proteome Analysis of Peroxisomes from Etiolated Arabidopsis Seedlings Identifies a Peroxisomal Protease Involved in β-Oxidation and Development[1][C][W][OPEN]

**Sheng Quan[2], Pingfang Yang[2,3], Gaëlle Cassin-Ross[2], Navneet Kaur[2], Robert Switzenberg, Kyaw Aung, Jiying Li, and Jianping Hu***

Department of Energy Plant Research Laboratory (S.Q., P.Y., G.C.-R., N.K., R.S., K.A., J.L., J.H.) and Plant Biology Department (K.A., J.H.), Michigan State University, East Lansing, Michigan 48824

Plant peroxisomes are highly dynamic organelles that mediate a suite of metabolic processes crucial to development. Peroxisomes in seeds/dark-grown seedlings and in photosynthetic tissues constitute two major subtypes of plant peroxisomes, which had been postulated to contain distinct primary biochemical properties. Multiple in-depth proteomic analyses had been performed on leaf peroxisomes, yet the major makeup of peroxisomes in seeds or dark-grown seedlings remained unclear. To compare the metabolic pathways of the two dominant plant peroxisomal subtypes and discover new peroxisomal proteins that function specifically during seed germination, we performed proteomic analysis of peroxisomes from etiolated Arabidopsis (*Arabidopsis thaliana*) seedlings. The detection of 77 peroxisomal proteins allowed us to perform comparative analysis with the peroxisomal proteome of green leaves, which revealed a large overlap between these two primary peroxisomal variants. Subcellular targeting analysis by fluorescence microscopy validated around 10 new peroxisomal proteins in Arabidopsis. Mutant analysis suggested the role of the cysteine protease RESPONSE TO DROUGHT21A-LIKE1 in β-oxidation, seed germination, and growth. This work provides a much-needed road map of a major type of plant peroxisome and has established a basis for future investigations of peroxisomal proteolytic processes to understand their roles in development and in plant interaction with the environment.

Peroxisomes, originally known as microbodies, are small and single-membrane eukaryotic organelles that compartmentalize various oxidative metabolic functions. Most peroxisomal matrix proteins carry a C-terminal tripeptide named PEROXISOME TARGETING SIGNAL TYPE1 (PTS1), and fewer contain an N-terminal nonapeptide, PTS2 (Lanyon-Hogg et al., 2010). PTS1 is further divided into major and minor PTS1s. Major PTS1 tripeptides, such as SKL> and SRL> (> represents the stop codon), are by themselves sufficient to direct a protein to the peroxisome (Reumann, 2004), whereas minor PTS1s are usually found in low-abundance proteins and require additional upstream elements for peroxisomal targeting (Kaur et al., 2009). Peroxisomes are highly variable morphologically and metabolically, as their size, shape, abundance, and enzymatic content can differ depending on the species, tissue and cell type, and prevailing environmental conditions (Beevers, 1979; van den Bosch et al., 1992; Kaur et al., 2009; Hu et al., 2012; Schrader et al., 2012).

Plant peroxisomes participate in a wide range of metabolic processes, such as lipid metabolism, photorespiration, detoxification, biosynthesis of jasmonic acid, and metabolism of indole-3-butyric acid (IBA), nitrogen, sulfite, and polyamine (Kaur et al., 2009; Hu et al., 2012). Specific names had been given to certain types of peroxisomes due to their unique metabolic properties. For example, the term glyoxysome was coined when a new type of organelle that contained enzymes of the glyoxylate cycle was identified from the endosperm of castor bean (*Ricinus communis*; Breidenbach et al., 1968). It was later realized that glyoxysomes are in fact a type of peroxisome, and Beevers (1979) subsequently classified plant peroxisomes into three subtypes based on their primary biochemical functions. Glyoxysomes are located in storage organs such as fatty seedling tissues and play a major role in converting fatty acids to sugar; leaf peroxisomes are involved in photorespiration; and nonspecialized peroxisomes exist in other plant tissues and perform unknown functions.

The primary function of leaf peroxisomes is the recycling of phosphoglycolate during photorespiration, a process coordinated by chloroplasts, peroxisomes, mitochondria, and the cytosol. In this pathway, phosphoglycolate

[1] This work was supported by the National Science Foundation Arabidopsis 2010 Program (grant no. MCB 0618335 to J.H.) and the Chemical Sciences, Geosciences, and Biosciences Division, Office of Basic Energy Sciences, Office of Science, U.S. Department of Energy (grant no. DE–FG02–91ER20021 to J.H.).

[2] These authors contributed equally to the article.

[3] Present address: Wuhan Botanical Garden, Chinese Academy of Sciences, Wuhan, China 430074.

* Address correspondence to huji@msu.edu.

The author responsible for distribution of materials integral to the findings presented in this article in accordance with the policy described in the Instructions for Authors (www.plantphysiol.org) is: Jianping Hu (huji@msu.edu).

[C] Some figures in this article are displayed in color online but in black and white in the print edition.

[W] The online version of this article contains Web-only data.

[OPEN] Articles can be viewed online without a subscription.

www.plantphysiol.org/cgi/doi/10.1104/pp.113.223453

 

produced by the oxygenase activity of Rubisco is ultimately converted to glycerate, which reenters the chloroplastic Calvin-Benson cycle (Foyer et al., 2009; Peterhansel et al., 2010). The peroxisome-localized enzymes glycolate oxidase (GOX), catalase, aminotransferase (serine:glyoxylate aminotransferase [SGT] and glutamate-glyoxylate aminotransferase [GGT]), HYDROXYPYRUVATE REDUCTASE1 (HPR1), and peroxisomal malate dehydrogenase (PMDH) are involved in the process (Reumann and Weber, 2006). On the other hand, lipid mobilization through fatty acid $\beta$-oxidation and the glyoxylate cycle is the main function for peroxisomes in seeds and germinating seedlings. In this process, fatty acids are first activated into fatty acyl-CoA esters by the acyl-activating enzyme (AAE)/acyl-CoA synthetase before entering the $\beta$-oxidation cycle, during which an acetyl-CoA is cleaved in each cycle by the successive action of acyl-CoA oxidase (ACX), multifunctional protein (MFP), and 3-keto-acyl-CoA thiolase (KAT). Acetyl-CoA, an end product of $\beta$-oxidation, is further converted to four-carbon carbohydrates by the glyoxylate cycle, in which isocitrate lyase (ICL) and malate synthase (MLS) are two key enzymes that function exclusively in this pathway. Products of the glyoxylate cycle exit the peroxisome, enter gluconeogenesis, and are further converted to hexose and Suc to fuel the postgerminative development of seedlings (Penfield et al., 2006).

Immunocytochemical studies of germinating seeds from pumpkin (*Cucurbita pepo*), watermelon (*Citrullis vulgaris*), and cucumber (*Cucumis sativus*) demonstrated that seed peroxisomes (glyoxysomes) are directly transformed into leaf peroxisomes during greening of the cotyledons without de novo biogenesis of leaf peroxisomes (Titus and Becker, 1985; Nishimura et al., 1986; Sautter, 1986). This conversion was illustrated by the import of photorespiratory enzymes and their concomitant presence with glyoxylate cycle enzymes within the same organelle. Furthermore, the increase in abundance of photorespiratory enzymes coincided with the marked decrease, and subsequently the absence, of glyoxylate cycle enzymes (ICL and/or MLS) at the culmination of this process (Titus and Becker, 1985; Nishimura et al., 1986; Sautter, 1986). It was suggested that the specific names for plant peroxisomal variants should be eliminated because protein composition between leaf peroxisomes and glyoxysomes may differ by only two proteins (i.e. ICL and MLS) out of the over 100 total proteins in the peroxisome (Pracharoenwattana and Smith, 2008). This prediction needed to be tested. In addition, mutants lacking core peroxisome biogenesis factors or major $\beta$-oxidation enzymes are nonviable, suggesting that peroxisomes are essential to embryogenesis and seed germination (Hu et al., 2012). However, how peroxisomes contribute to seed germination and seedling establishment is not completely understood. In the past, studies have been successfully undertaken to catalog the proteome of mitochondria and plastids isolated from different plant tissues, which uncovered unique facets of organelle metabolism in various tissues (van Wijk and Baginsky, 2011; Havelund et al., 2013; Lee et al., 2013). As such, it was necessary to establish a protein atlas for peroxisomes in dark-grown seedlings.

Proteomic analyses of leaf peroxisomes and peroxisomes from suspension-cultured, leaf-derived cells followed by protein subcellular localization studies confirmed a total of over 30 new peroxisomal proteins, uncovering additional metabolic functions for leaf peroxisomes (Fukao et al., 2002; Reumann et al., 2007, 2009; Eubel et al., 2008; Babujee et al., 2010; Kataya and Reumann, 2010; Quan et al., 2010). For Arabidopsis (*Arabidopsis thaliana*), around 100 peroxisomal proteins were shown to be present in leaves or leaf-derived cells. Compared with the over 80 bona fide peroxisomal proteins detected by leaf peroxisomal proteomics (Reumann et al., 2007, 2009), the number of proteins identified from peroxisomal proteomic studies on etiolated seedlings was significantly smaller, with less than 10 known peroxisomal proteins from Arabidopsis (Fukao et al., 2003) and approximately 31 from soybean (*Glycine max*; Arai et al., 2008a, 2008b). Thus, a more in-depth analysis of the proteome of peroxisomes from these tissues was highly needed.

Here, we performed proteomic analysis of peroxisomes isolated from etiolated Arabidopsis seedlings and detected peroxisomal proteins that encompass most of the known plant peroxisomal metabolic pathways. Fluorescence microscopy verified the peroxisomal localization of a number of proteins newly identified in this study or detected from previous proteomics that had not been verified by independent means. Reverse genetic analysis demonstrated the role for a Cys protease in germination, $\beta$-oxidation, and growth.

## RESULTS

### Isolation of Peroxisomes from Etiolated Seedlings

To select a developmental stage that yields an adequate amount of tissue for organelle isolation but also coincides with the peak activity of peroxisomes, we monitored the activity of ICL, a marker enzyme for peroxisomes in seeds and early seedlings, in 3- to 6-d-old dark-grown Arabidopsis seedlings. Consistent with a previous report (Germain et al., 2001), the highest ICL activity was found to be present in 3-d-old seedlings (Supplemental Fig. S1), which were thus chosen for subsequent peroxisome isolation (Fig. 1A).

Peroxisome purification was performed using a protocol adopted from the two-density gradient centrifugation method developed for leaf peroxisomes (Reumann et al., 2007) and with some modifications of the Percoll and Suc concentrations (see "Materials and Methods"). Pellet from the Percoll gradient, which contained peak activity of ICL (Fig. 1B, fraction 14), was washed and loaded onto the Suc gradient (Fig. 1C). A distinctive white band was observed in the 51% (w/v) Suc after the second gradient centrifugation, which is similar to what we normally see for leaf peroxisome isolation

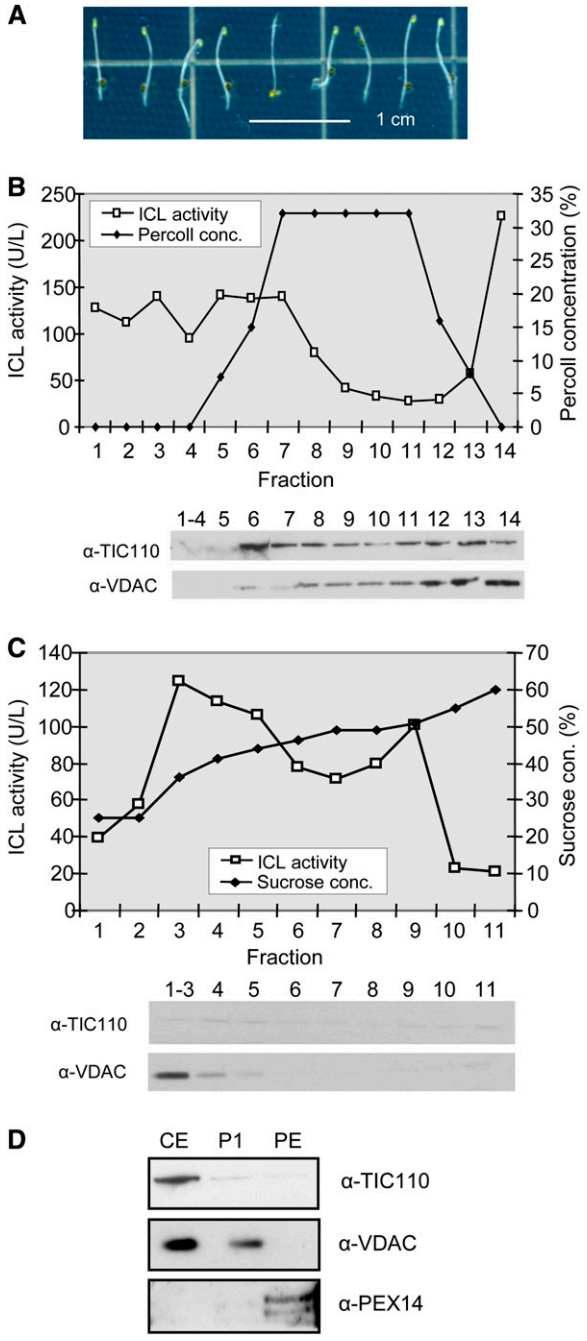


**Figure 1.** Isolation of peroxisomes from etiolated Arabidopsis seedlings. A, Image of 3-d-old dark-grown seedlings. B and C, Measurement of ICL activity and detection of chloroplast and mitochondrial contaminants in various fractions in Percoll (B) and Suc (C) density gradient centrifugations. The number label for each lane of the immunoblots correlates to the number of the fraction shown in the associated graph. D, Immunoblot analysis of approximately 10 $\mu$g of protein each from crude extracts (CE), pellet fraction after Percoll gradient centrifugation (fraction 14 in Fig. 2B; P1), and highly enriched peroxisomes obtained after Suc gradient centrifugation (fraction 9 in Fig. 2C; PE). For immunoblots, proteins were separated on an SDS-PAGE gel and detected by antibodies against the following organelle membrane proteins: chloroplast TIC110, mitochondrial VDAC, and peroxisomal PEX14 proteins. [See online article for color version of this figure.]

(Reumann et al., 2007, 2009). To ascertain the composition of this band, immunoblot analysis was performed on proteins from crude extract, pellet fraction (P1) after Percoll gradient centrifugation (fraction 14 in Fig. 1B), and the fraction that contained the white band (PE) after Suc gradient centrifugation (fraction 9 in Fig. 1C; Supplemental Fig. S2) using organelle-specific antibodies (Fig. 1D). Antibodies against the chloroplast inner envelope protein TIC110 from pea (*Pisum sativum*) and the mitochondrial outer membrane-localized voltage-dependent anion-selective channel protein (VDAC) from maize (*Zea mays*) detected minimal presence of these proteins (112 and 30 kD, respectively) in the PE fraction compared with crude exact and P1 (Fig. 1D). In contrast, antibodies against the Arabidopsis peroxisomal membrane protein PEX14 revealed a high enrichment of this protein in the PE fraction (Fig. 1D). Interestingly, $\alpha$-PEX14, which detected a single band of approximately 75 kD in 8-d-old light-grown seedlings (Monroe-Augustus et al., 2011), consistently detected two bands around approximately 75 kD in the etiolated samples (Fig. 1D). This pattern is similar to what was observed for the phosphorylated PEX14 proteins in the yeasts *Pichia pastoris* (Johnson et al., 2001; Johnson and Olsen, 2001) and *Hansenula polymorpha* (Komori et al., 1999). Although whether this doublet is associated with protein phosphorylation has not yet been confirmed, Arabidopsis PEX14 has been found to be phosphorylated by multiple phosphoproteomic studies (Sugiyama et al., 2008; Jones et al., 2009; Reiland et al., 2009, 2011; Nakagami et al., 2010; Wang et al., 2013).

As a second line of confirmation, we also measured ICL activity in various fractions of the two gradients after centrifugation (Fig. 1, B and C). As expected, the PE fraction possessed a peak activity of ICL. In contrast, fraction 3 of the Suc gradient, which showed another peak ICL activity, had much higher contamination from mitochondria, as evidenced by the detection of a strong VDAC band on the immunoblot (Fig. 1C). Fraction 3 was thus considered to contain broken peroxisomes.

These results together suggested that our isolation procedure was successful in obtaining a fraction containing highly enriched peroxisomes that was fairly well separated from plastids and mitochondria. Consistent with previous reports on Arabidopsis leaf peroxisomes (Reumann et al., 2007, 2009), fraction 9 of the Suc gradient contained highly enriched peroxisomes and was collected from subsequent peroxisomal preparations.

### One-Dimensional Gel Electrophoresis Followed by Liquid Chromatography-Tandem Mass Spectrometry-Based Identification of Peroxisomal Proteins

After purity assessment by immunoblots, peroxisomal samples were subjected to one-dimensional gel electrophoresis (1-DE) followed by liquid chromatography-tandem mass spectrometry (LC-MS/MS). To maximize the coverage of peroxisomal proteins, we employed three different approaches for protein separation. First,

approximately 200 $\mu$g of total peroxisomal proteins was separated in a single lane on an SDS-PAGE gel, which was later cut into 10 slices. From two biological replicates (named T1 and T2), we identified 147 and 135 proteins, respectively (Supplemental Tables S1 and S2). In the second approach, we used a ZOOM IEF Fractionator (Invitrogen), a solution-phase isoelectric focusing apparatus that can divide total proteins into different subgroups based on each protein's pI, in an attempt to identify low-abundance proteins that might have been masked by abundant proteins in the same gel lane in the first approach. Approximately 800 $\mu$g of peroxisomal proteins combined from three to four preparations was fractionated into five pH groups: 3.0 to 4.6 (Z1), 4.6 to 5.4 and 5.4 to 6.2 (later combined as Z2), 6.2 to 7.0 (Z3), and 7.0 to 10.0 (Z4). Proteins were then separated by 1-DE before each gel lane was cut into three to five slices depending on the amount of proteins in the lane. Totals of 85, 147, 72, and 108 proteins were identified from Z1 to Z4, respectively (Supplemental Tables S3–S6). In the third experiment, we enriched the peroxisomal membrane fraction by treating approximately 600 $\mu$g of total peroxisomal proteins combined from two to three preparations with 100 mM $Na_2CO_3$ and used the membrane-enriched sample for 1-DE, after which the gel lane was sliced into eight pieces. A total of 55 proteins was detected from this fraction (Supplemental Table S7).

Out of the proteins identified from T1 and T2, 29% (T1) and 31% (T2) were known to be peroxisomal; thus, there were still significant numbers of proteins from other subcellular compartments, most notably plastids and the secretory system, which had been copurified with peroxisomes (Supplemental Fig. S3). To evaluate the enrichment of peroxisomes more precisely, the relative abundance of proteins assigned to various subcellular organelles was compared using quantitative value (QV). These values were derived from normalized spectral abundance factors, which normalize spectral counts according to the length of each protein and variation between sample runs (Paoletti et al., 2006). Peroxisomal proteins accounted for 61% in T1 and 71% in T2 of the total proteins (Fig. 2, A and B). Notably, subcellular distribution as well as spectral count-based quantification of peroxisomal proteins in this study are comparable to the data reported for peroxisomes isolated from human liver tissue (Gronemeyer et al., 2013a). ZOOM fractionation before 1-DE allowed us to detect 26 additional peroxisomal proteins that were undetected in T1 and T2, including two new peroxisomal proteins later verified in this study (see below), and therefore significantly improved the coverage of the peroxisomal proteome (Fig. 2C). From the peroxisomal membrane, we identified 31 peroxisomal proteins, including integral membrane proteins such as the ATP-binding cassette transporter PXA1/CTS/PED3 and PEROXIN11a (PEX11a), that were undetected in the total peroxisomal samples using the first two approaches.

Altogether, 77 true peroxisomal proteins were identified from etiolated seedling peroxisomes (Table I), including the 11 proteins later validated in this study. These proteins covered all those identified from previous proteome studies of etiolated seedlings except for GLYOXYSOMAL PROTEIN KINASE1 plus an additional 53 proteins, representing more than 3-fold improvement over previous peroxisomal proteome studies of the same tissue (Fig. 2D).

### Validation of New Peroxisomal Proteins by Fluorescence Microscopy

To identify new peroxisomal proteins and reveal previously unknown peroxisomal functions of etiolated seedlings, we selected candidate proteins for in vivo subcellular targeting analysis. First, for each protein on our list of nonredundant proteins identified from this study, we queried the Arabidopsis Subcellular Database SUBA3 (Tanz et al., 2013) to retrieve data regarding fluorescent protein localization, identification in prior proteomics studies, and predicted localization (Supplemental Table S8). Using this information, we excluded proteins that had experimentally proven nonperoxisomal fluorescent protein localization or had been repeatedly isolated from proteomics studies of other organelles. The remaining 36 candidates were tested for subcellular localization (Supplemental Table S4). Among them, ACAT2-GFP had been found to be cytosolic in a previous study but the C terminus was blocked in the fusion protein (Carrie et al., 2007), and BADH was shown to target to punctate structures without a peroxisomal marker as a reference (Missihoun et al., 2011). Thus, these two proteins were retested in our study.

To express proteins under the control of the *CaMV35S* promoter, the coding region of each candidate gene was fused to enhanced yellow fluorescent protein (YFP) in the Gateway-compatible destination vectors generated in our previous study (Reumann et al., 2009). Proteins containing C-terminal PTS1 or PTS1-like sequences were fused to the C terminus of YFP, proteins with N-terminal PTS2 or PTS2-like sequences were fused to the N terminus of YFP, and those without recognizable PTS were cloned in both orientations. Since minor PTS1s in plants are very diverse, here we classified proteins with C-terminal tripeptides that differed by one amino acid from the high-targeting-strength residues [SA][KR][LMI] (Lingner et al., 2011) as PTS1-like. We used tobacco (*Nicotiana tabacum*) leaves to transiently coexpress the YFP fusion proteins and the peroxisomal marker cyan fluorescent protein-PTS1 (SKL). Two days after inoculation of agrobacteria containing the constructs, confocal laser scanning microscopy was performed to examine the subcellular localization of the fusion proteins in leaf epidermal cells.

Six proteins that contained PTS or PTS-like sequences and had also been identified from previous peroxisomal proteomics but not validated, ACYL-ACTIVATING ENZYME5 (AAE5), SHORT-CHAIN DEHYDROGENASE/REDUCTASE ISOFORM d (SDRd), COBALAMIN-INDEPENDENT METHIONINE SYNTHASE1 (ATMS1),

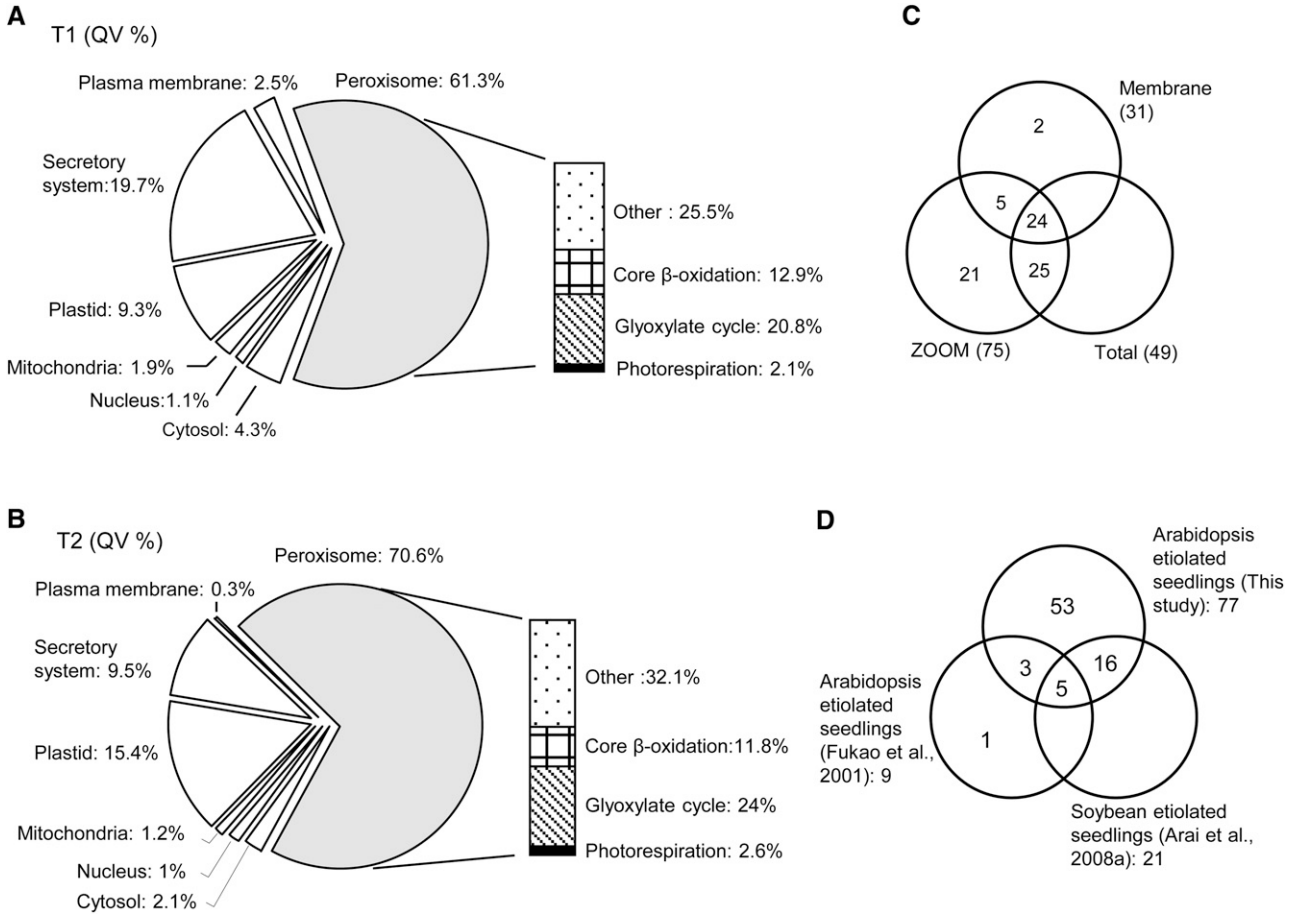


**Figure 2.** Subcellular distribution of proteins identified from total peroxisomes in this study and comparison of the number of peroxisomal proteins identified by different methods and from different studies. A and B, Relative abundance (QV %) of proteins in various subcellular compartments identified from the two total peroxisome samples, T1 (A) and T2 (B). Among the peroxisomal proteins, the abundance of proteins involved in core fatty acid $\beta$-oxidation, glyoxylate cycle, and photorespiration are compared. C and D, Comparison of the number of peroxisomal proteins identified by different methods in this study (C) and from three independent studies (D).

GLYCOLATE OXIDASE ISOFORM3 (GOX3), a protein with unknown function (UP3), and BETAINE ALDEHYDE DEHYDROGENASE (BADH), colocalized with the peroxisomal marker (Supplemental Fig. S4). Out of the proteins that contained PTS or PTS-like sequences and were only identified in this proteomic study, four of them, BENZOYLOXYGLUCOSINOLATE1/BENZOATE-COENZYME A LIGASE (BZO1; At1g65880, SRL>), an ortholog of petunia (*Petunia hybrida*) PhCNL (Lee et al., 2012), SERINE CARBOXYPEPTIDASE-LIKE20 (SCPL20; At4g12910, SKI >), the papain-like Cys proteinase RD21A-LIKE PROTEASE1 (RDL1; At4g36880, SSV>), and a protein with unknown function (UP9; At1g29120, ASL>), were localized to peroxisomes when fused to the C terminus of YFP (Fig. 3, A–D). Interestingly, YFP-BZO1 appeared to encircle the peroxisome in the form of a narrow strip at the center of the organelle (Fig. 3D). In contrast, none of the proteins that contained no recognizable PTS or PTS-like sequences were found to be peroxisome localized (Supplemental Table S9).

Considering the presence of dual-localized peroxisomal proteins (Carrie et al., 2007, 2009a, 2010; Aung and Hu, 2011, 2012), we also reanalyzed a few proteins that had been categorized as contaminants in previous proteomic works. Comparing our list of identified proteins with listed contaminants from previously conducted peroxisome proteomics experiments, we short listed five proteins that had the potential to be dual localized. Among them, GLYCERALDEHYDE 3-PHOSPHATE DEHYDROGENASE C2 (GAPC2) had a PTS1-like sequence (SKA>) and 2-CYS PEROXIREDOXIN had a putative PTS2 (RVxSL). Rab GTPase homolog E1b was included because of the reported association of Rab proteins with peroxisomes in both plant and mammalian systems (Schollenberger et al., 2010; Cui et al., 2013; Gronemeyer et al., 2013b). Glutathione *S*-transferase $\phi$8 was chosen, given that some of the glutathione *S*-transferase isoforms detected in plant peroxisome proteomic experiments had been confirmed to be peroxisomal by localization studies

**Table I.** *List of peroxisomal proteins identified from Arabidopsis etiolated seedlings in this study*

T1, T2, Z, and M stand for total proteomics 1 and 2, ZOOM, and membrane proteomics, respectively. MM, Predicted molecular mass (in kD). For T1 and T2, QV, percentage coverage (P), and number of unique peptides (N) are presented. Individual proteomics experimental details can be found in Supplemental Tables S1 to S7. The entire list of nonredundant proteins identified across seven experiments is presented in Supplemental Table S8. Numbers refer to previously conducted plant peroxisome proteomics experiments, where 1 to 8 refer to Eubel et al. (2008), Reumann et al. (2007), Reumann et al. (2009), Fukao et al. (2002), Fukao et al. (2003), Arai et al. (2008a), Arai et al. (2008b), and Babujee et al. (2010), respectively. Asterisks indicate newly identified peroxisomal proteins, and Y indicates proteins validated to be peroxisomal by subcellular targeting in this study. x, Presence; −, absence.

| Annotation | Locus | Symbol | MM | pI | PTS1/PTS2 | T1 | QV | P | N | T2 | QV | P | N | Z | M | 1 | 2 | 3 | 4 | 5 | 6 | 7 | 8 |
|---|---|---|---|---|---|---|---|---|---|---|---|---|---|---|---|---|---|---|---|---|---|---|---|
| Glyoxylate cycle | | | | | | | | | | | | | | | | | | | | | | | |
| Citrate synthase3 | At2g42790 | CSY3 | 56 | 7.8 | SSV/RLxHL | x | 83.3 | 45 | 23 | x | 31.5 | 33 | 17 | x | x | x | x | x | − | − | x | − | − |
| Isocitrate lyase | At3g21720 | ICL | 64 | 7.2 | SRM | x | 443.4 | 48 | 25 | x | 477.9 | 50 | 28 | x | x | − | − | − | − | x | x | x | x |
| Citrate synthase2 | At3g58750 | CSY2 | 57 | 8.9 | SAL/RLxHL | x | 18.4 | 25 | 5 | x | 5.8 | 15 | 3 | x | x | x | − | x | − | − | − | − | x |
| Malate synthase | At5g03860 | MLS | 64 | 8 | SRL | x | 192.1 | 41 | 27 | x | 273.1 | 43 | 29 | x | x | − | − | − | − | x | x | x | x |
| Core β-oxidation related | | | | | | | | | | | | | | | | | | | | | | | |
| 3-Ketoacyl-CoA thiolase1 | At1g04710 | KAT1 | 47 | 8.4 | RQxHL | | | | | | | | | x | | x | x | x | − | − | − | − | − |
| Acyl-CoA oxidase3 | At1g06290 | ACX3 | 76 | 8.1 | SSV/RAxHI | x | 33.5 | 12 | 11 | x | 24.1 | 15 | 13 | x | | x | x | x | − | − | − | − | − |
| 3-Ketoacyl-CoA thiolase2 | At2g33150 | KAT2 | 49 | 8.5 | RQxHL | x | 169.3 | 69 | 26 | x | 105.4 | 55 | 22 | x | x | x | x | x | − | x | x | | x |
| Long-chain acyl-CoA synthetase6 | At3g05970 | LACS6 | 77 | 8 | RIxHL | x | 14 | 13 | 8 | x | 5.3 | 3.3 | 2 | x | x | x | − | x | − | − | − | − | x |
| Fatty acid multifunctional protein2 | At3g06860 | MFP2 | 79 | 9.7 | SRL | x | 134.3 | 51 | 37 | x | 128.7 | 30 | 28 | x | x | x | x | x | − | − | x | x | − |
| Acyl-CoA oxidase4 | At3g51840 | ACX4 | 48 | 8.5 | SRL | x | 11.5 | 23 | 7 | x | 20.6 | 17 | 7 | x | | x | x | x | − | − | x | x | − |
| Monofunctional enoyl-CoA hydratase/isomerase a | At4g16210 | ECHIA | 29 | 9.7 | SKL | x | 12.7 | 42 | 10 | x | 27.5 | 42 | 12 | x | x | x | x | x | − | − | x | − | x |
| Acyl-CoA oxidase1 | At4g16760 | ACX1 | 74 | 7.7 | ARL | x | 58.6 | 27 | 16 | x | 68.1 | 28 | 20 | x | | x | − | x | − | − | − | x | − |
| Abnormal inflorescence meristem1 | At4g29010 | AIM1 | 78 | 9.9 | SKL | x | 10.1 | 10 | 7 | x | 3.5 | 4.9 | 4 | x | x | x | x | x | − | − | − | − | − |
| Long-chain acyl-CoA synthetase7 | At5g27600 | LACS7 | 77 | 6.6 | SKL/RLxHI | x | 3.4 | 5.1 | 2 | | | | | x | x | x | x | x | − | − | − | x | − |
| Δ3,5-Δ2,4-Enoyl-CoA isomerase | At5g43280 | AtDCI | 30 | 7.9 | AKL | | | | | | | | | x | | x | x | x | − | − | − | − | − |
| Acyl-CoA oxidase2 | At5g65110 | ACX2 | 77 | 8.4 | RIxHL | x | 8.2 | 12 | 7 | x | 5.6 | 8.4 | 6 | x | x | − | − | x | − | − | − | − | − |
| Auxiliary β-oxidation related | | | | | | | | | | | | | | | | | | | | | | | |
| Short-chain dehydrogenase/reductase c | At3g01980 | SDRc | 29 | 7.8 | SYM | | | | | | | | | x | | − | x | x | − | − | − | − | − |
| Short-chain dehydrogenase/reductase b | At3g12800 | SDRb | 32 | 9.6 | SKL | x | 5.2 | 14 | 3 | x | 10.3 | 17 | 5 | x | | x | x | x | − | − | − | − | − |
| Hydroxybutyryl-CoA dehydrogenase | At3g15290 | HBCDH | 32 | 7.1 | PRL | | | | | x | 3.9 | 13 | 4 | x | | x | x | x | − | − | x | − | − |
| Short-chain dehydrogenase/reductase | At3g55290 | SDRd[Y] | 30 | 8.4 | SSL | x | 7.8 | 26 | 6 | x | 16 | 27 | 7 | x | | x | x | x | − | − | − | − | − |
| Acyl-activating enzyme5 | At5g16370 | AAE5[Y] | 61 | 7 | SRM | | | | | | | | | x | x | x | x | x | − | − | − | − | − |
| Sterol carrier protein2 | At5g42890 | SCP2 | 14 | 9.9 | SKL | x | 32.5 | 77 | 13 | x | 19.7 | 66 | 7 | x | | x | x | x | − | − | − | − | − |
| IBA related | | | | | | | | | | | | | | | | | | | | | | | |
| Monofunctional enoyl-CoA hydratase2 | At1g76150 | ECH2 | 34 | 7.4 | SSL | x | 5.7 | 17 | 5 | x | 10.3 | 21 | 6 | x | | x | x | x | − | − | − | − | − |
| Indole-3-butyric acid3 | At3g06810 | IBR3 | 92 | 8.5 | SKL | | | | | | | | | x | x | x | − | x | − | − | − | − | − |
| Indole-3-butyric acid response1 | At4g05530 | IBR1 | 27 | 8.7 | SRL | x | 6.4 | 28 | 5 | x | 17.5 | 32 | 7 | x | | x | x | x | − | − | x | − | x |
| Indole-3-butyric acid response10 | At4g14430 | IBR10 | 26 | 8.7 | PKL | | | | | x | 3.7 | 9.6 | 2 | x | | x | x | x | − | − | − | − | − |
| Jasmonate biosynthesis | | | | | | | | | | | | | | | | | | | | | | | |
| 12-Oxophytodienoate reductase3 | At2g06050 | OPR3 | 43 | 8 | SRL | x | 11.4 | 15 | 8 | x | 2.3 | 5.4 | 2 | x | | x | x | x | − | − | − | − | x |
| 4-Coumarate:CoA ligase1 | At4g05160 | 4CLP1 | 60 | 8.7 | SKM | | | | | | | | | x | x | x | x | x | − | − | − | − | − |
| BA biosynthesis | | | | | | | | | | | | | | | | | | | | | | | |
| Benzoyloxyglucosinolate1 | At1g65880 | BZO1*[Y] | 65 | 7.7 | SRL | | | | | | | | | x | | − | − | − | − | − | − | − | − |
| CoA regeneration | | | | | | | | | | | | | | | | | | | | | | | |
| Acyl-CoA thioesterase | At1g01710 | ACH2 | 48 | 7.6 | SKL | | | | | | | | | x | | x | x | x | x | − | − | − | − |
| Small thioesterase3 | At3g61200 | sT3 | 20 | 6.8 | SKL | | | | | | | | | x | | x | − | x | − | x | − | − | − |
| Photorespiration | | | | | | | | | | | | | | | | | | | | | | | |
| Glu-glyoxylate aminotransferase1 | At1g23310 | GGT1 | 53 | 6.9 | SKM | | | | | x | 2.2 | 4.4 | 3 | x | | x | x | x | x | − | − | − | x |

(*Table continues on following page.*)

**Table I.** (*Continued from previous page.*)

| Annotation | Locus | Symbol | MM | pI | PTS1/PTS2 | T1 | QV | P | N | T2 | QV | P | N | Z | M | 1 | 2 | 3 | 4 | 5 | 6 | 7 | 8 |
|---|---|---|---|---|---|---|---|---|---|---|---|---|---|---|---|---|---|---|---|---|---|---|---|
| Hydroxypyruvate reductase1 | At1g68010 | HPR1 | 42 | 7.2 | SKL | x | 1.9 | 5.2 | 2 | x | 3.9 | 11 | 4 | x | | x | x | x | x | – | x | – | x |
| Glu-glyoxylate aminotransferase2 | At1g70580 | GGT2 | 53 | 6.5 | SRM | x | 3.6 | 12 | 4 | | | | | x | | x | x | x | x | – | – | – | – |
| Glycolate oxidase1 | At3g14415 | GOX1 | 40 | 9.4 | PRL | x | 42.2 | 44 | 20 | x | 57.5 | 43 | 20 | x | x | x | x | x | x | – | x | – | x |
| Glycolate oxidase2 | At3g14420 | GOX2 | 40 | 9.6 | ARL | x | 26.6 | 33 | 3 | x | 22.5 | 34 | 4 | x | | x | x | x | x | – | x | – | x |
| Glycolate oxidase3 | At4g18360 | GOX3[Y] | 40 | 8.6 | AKL | | | | | | | | | x | | x | x | x | – | – | – | – | – |
| Phylloquinone biosynthesis | | | | | | | | | | | | | | | | | | | | | | | |
| Naphthoate synthase | At1g60550 | NS | 37 | 7.3 | RLxHL | | | | | | | | | x | | – | x | x | – | – | – | – | x |
| Small thioesterase1 | At1g48320 | sT1 | 17 | 9.4 | AKL | | | | | | | | | x | | – | – | x | – | – | – | – | – |
| Detoxification | | | | | | | | | | | | | | | | | | | | | | | |
| Catalase3 | At1g20620 | CAT3 | 57 | 7.7 | – | x | 408.3 | 61 | 26 | x | 499.6 | 67 | 32 | x | x | x | x | x | x | x | – | – | x |
| Catalase1 | At1g20630 | CAT1 | 57 | 7.4 | – | x | 28.2 | 26 | 4 | x | 36.5 | 25 | 4 | x | | x | x | x | – | – | – | – | x |
| Ascorbate peroxidase3 | At4g35000 | APX3 | 32 | 7 | – | x | 27.7 | 48 | 16 | x | 38.7 | 52 | 15 | x | x | x | x | x | x | x | x | x | x |
| Catalase2 | At4g35090 | CAT2 | 57 | 7.1 | – | x | 157.4 | 55 | 18 | x | 136.5 | 47 | 17 | x | | x | x | x | x | – | x | x | x |
| Copper/zinc superoxide dismutase3 | At5g18100 | CSD3 | 17 | 7.7 | AKL | x | 6.7 | 21 | 3 | x | 2.6 | 13 | 2 | x | | – | x | x | – | – | – | – | – |
| Glutathione *S*-transferase $\theta$-isoform1 | At5g41210 | GSTT1 | 28 | 10 | SKI | x | 7.4 | 12 | 3 | x | 25.4 | 29 | 9 | x | x | x | x | x | – | – | – | – | – |
| NADH/NADPH regeneration | | | | | | | | | | | | | | | | | | | | | | | |
| Glyceraldehyde 3-phosphate dehydrogenase C2 | At1g13440 | GAPC2*[Y] | 37 | 7.2 | SKA | | | | | x | 3.3 | 7.1 | 3 | x | x | x | – | – | – | – | – | – | – |
| NADH:quinone reductase | At1g49670 | NQR | 68 | 9.5 | SRL | | | | | | | | | x | x | x | x | x | – | – | – | – | – |
| NADP-dependent isocitrate dehydrogenase | At1g54340 | ICDH | 47 | 7.8 | SRL | | | | | | | | | x | | x | x | x | – | x | – | – | – |
| Peroxisomal NAD malate dehydrogenase1 | At2g22780 | PMDH1 | 37 | 8.1 | RIxHL | x | 26.2 | 39 | 12 | x | 23.6 | 36 | 11 | x | x | x | x | x | x | x | x | – | x |
| Phosphogluconate dehydrogenase | At3g02360 | 6PGDH | 54 | 7.5 | SKI | | | | | | | | | x | | x | x | x | – | – | – | – | – |
| Zinc-binding dehydrogenase | At3g56460 | ZnDH | 37 | 9.7 | SKL | | | | | | | | | x | | x | – | x | – | – | – | – | – |
| Peroxisomal NAD malate dehydrogenase2 | At5g09660 | PMDH2 | 37 | 8.1 | RIxHL | x | | | | | | | | x | | x | x | x | x | – | x | – | x |
| Sulfur and nitrogen metabolism | | | | | | | | | | | | | | | | | | | | | | | |
| Indigoidine synthase A | At1g50510 | IndA | 35 | 7.6 | RIxHL | x | 12.9 | 19 | 5 | x | 4.2 | 6.1 | 3 | x | x | x | – | x | – | – | – | – | – |
| Uricase | At2g26230 | Uri | 35 | 8.7 | SKL | | | | | | | | | x | | x | x | x | – | – | x | – | x |
| Copper amine oxidase | At2g42490 | CuAO | 87 | 7.1 | SKL | | | | | | | | | x | | x | – | x | – | – | – | – | – |
| Sulfite oxidase | At3g01910 | SO | 43 | 9 | SNL | x | 4.8 | 7.1 | 2 | x | 12.2 | 23 | 9 | x | | x | x | x | – | – | – | – | x |
| Aldehyde dehydrogenase | At3g48170 | BADH | 55 | 5.2 | SKL | | | | | | | | | x | | x | x | x | – | – | x | – | – |
| Asp aminotransferase | At5g11520 | ASP3 | 49 | 9.7 | RIxHL | x | 52.8 | 51 | 19 | x | 124.3 | 38 | 17 | x | x | x | x | x | x | – | x | – | x |
| Cobalamin-independent Met synthase1 | At5g17920 | ATMS1[Y] | 84 | 6.5 | SAK | x | 6.9 | 5.8 | 4 | x | 6.1 | 7.6 | 5 | x | | – | x | x | – | – | – | – | – |
| Proteases and chaperones | | | | | | | | | | | | | | | | | | | | | | | |
| Ser carboxypeptidase-like20 | At4g12910 | SCPL20*[Y] | 56 | 6.2 | SKI | x | 32.1 | 16 | 11 | x | 12.1 | 9.1 | 8 | x | | | | | | | | | |
| RD21A-like Cys protease1 | At4g36880 | RDL1*[Y] | 42 | 7.7 | SSV | x | 4.8 | 11 | 3 | | | | | x | | | | | | | | | |
| Heat shock protein similar to 17.6-kD class I | At5g37670 | AtHsp15.7 | 16 | 8.9 | SKL | | | | | | | | | x | | – | – | – | – | – | x | – | – |
| Lon protease homolog2 | At5g47040 | LON2 | 98 | 7.3 | SKL | | | | | x | 7.3 | 5.1 | 6 | x | x | – | – | x | – | – | – | – | – |
| Other functions | | | | | | | | | | | | | | | | | | | | | | | |
| Unknown protein6 | At1g16730 | UP6 | 22 | 4.8 | SKL | x | 11.6 | 54 | 9 | | | | | x | | – | – | x | – | – | – | – | – |
| Unknown protein9 | At1g29120 | UP9*[Y] | 50 | 10 | ASL | | | | | | | | | x | | – | – | – | – | – | – | – | – |
| Acetyltransferase | At1g77540 | ATF2 | 13 | 8.2 | SSI | | | | | | | | | x | | – | – | x | – | – | – | – | – |
| Unknown protein3 | At2g31670 | UP3[Y] | 29 | 7 | SSL | x | 4 | 8 | 2 | | | | | x | | – | x | x | – | – | – | – | – |
| Nucleoside diphosphate kinase type 1 | At4g09320 | NDPK1 | 19 | 8.5 | – | | | | | | | | | x | | – | – | x | – | – | – | – | – |
| His triad family protein1 | At4g16566 | HIT1 | 17 | 9.2 | SKV | | | | | | | | | x | | x | x | x | – | – | – | – | – |
| Acetoacetyl-CoA thiolase1.0.3 | At5g47720 | ACAT1.3 | 42 | 6.4 | SAL | | | | | | | | | x | | | | | | | | | |
| 3-Hydroxyisobutyryl-CoA hydrolase | At5g65940 | CHY1 | 42 | 8.3 | AKL | | | | | | | | | x | x | x | – | x | – | – | x | – | – |
| Biogenesis factors | | | | | | | | | | | | | | | | | | | | | | | |

(*Table continues on following page.*)

**Table I.** (*Continued from previous page.*)

| Annotation | Locus | Symbol | MM | pI | PTS1/PTS2 | T1 | QV | P | N | T2 | QV | P | N | Z | M | 1 | 2 | 3 | 4 | 5 | 6 | 7 | 8 |
|---|---|---|---|---|---|---|---|---|---|---|---|---|---|---|---|---|---|---|---|---|---|---|---|
| Peroxin11a | At1g47750 | PEX11a | 28 | 9.9 | – | | | | | | | | | | x | x | – | x | – | – | – | – | – |
| Peroxin11d | At2g45740 | PEX11d | 26 | 11 | – | x | 3 | 12 | 2 | x | 12.2 | 22 | 3 | x | x | x | x | x | – | – | – | – | – |
| Peroxin11e | At3g61070 | PEX11e | 26 | 11 | – | x | 4 | 13 | 2 | x | 19.6 | 33 | 9 | x | x | x | – | x | – | – | – | – | – |
| Peroxin14 | At5g62810 | PEX14 | 56 | 5.8 | – | x | 29.5 | 23 | 12 | | | | | x | x | x | x | x | – | – | – | – | – |
| Transport proteins | | | | | | | | | | | | | | | | | | | | | | | |
| Peroxisomal $NAD^+$ carrier | At2g39970 | PXN | 36 | 10 | – | | | | | x | 6.5 | 10 | 4 | x | x | x | – | x | – | – | – | – | – |
| Peroxisomal ATP-binding cassette transporter1 | At4g39850 | PXA1 | 150 | 9.3 | – | | | | | | | | | | x | x | – | x | – | – | – | – | – |

(Reumann et al., 2007, 2009; Eubel et al., 2008). Lastly, ASPARTATE AMINOTRANSFERASE2 was selected on the basis of the reported dual localization of another aminotransferase (Carrie et al., 2009b). Confocal imaging showed that out of the five proteins, only GAPC2 displayed colocalization with the peroxisome marker (Fig. 3E). Consistent with previous reports using GAPC2-YFP (Guo et al., 2012; Vescovi et al., 2013), we also observed strong cytosolic signals for YFP-GAPC2 (Fig. 3E).

Taken together, 11 of the 36 proteins tested were confirmed to be peroxisomal (Supplemental Table S9) and thus constituted new additions to Arabidopsis peroxisomal proteins (Table I). Seven proteins have been detected in peroxisomes isolated from leaves, cell cultures, and etiolated seedlings, while RDL1, SCPL20, UP9, and BZO1 were newly discovered in etiolated seedling peroxisomes (Table I). Since BZO1's function in benzoic acid (BA) biosynthesis has been shown (see "Discussion"), we searched for homologous sequences in other species for RDL1, SCPL20, and UP9, all of which contained well-established PTS1. Interestingly, we could only locate homologous sequences of these proteins in plant lineages, as opposed to GAPC2, whose orthologs in other eukaryotic systems had been characterized (see "Discussion"), suggesting that these three proteins may carry out plant-specific roles within peroxisomes. Amino acid sequence analyses revealed that all of these homologous sequences have conserved PTS1 or PTS1-like sequences, indicating that the corresponding proteins fulfill similar functions in plant peroxisomal metabolism (Fig. 4, A–C). GAPC2's homologous sequences from fungal genomes carry experimentally validated PTS1, but their homologous sequences in plants exhibited great diversity in the C-terminal tripeptide, most of which are PTS1-like (Fig. 4D).

### Peroxisomal Metabolic Pathways in Etiolated Seedlings

To analyze the metabolic events that occur in peroxisomes of etiolated seedlings, we compared the list of proteins identified in this study with those from two previously conducted major peroxisome proteomic investigations (Eubel et al., 2008; Reumann et al., 2009). Shared among the three peroxisomal proteomic experiments were 59 proteins that covered all the major biochemical processes associated with leaf peroxisomes, from $\beta$-oxidation and detoxification to photorespiration (Supplemental Table S10; Supplemental Fig. S5), suggesting that the core peroxisome proteome is largely conserved among peroxisomes from starkly different tissues.

From this study, only eight proteins appeared to be unique to (or much more abundant in) peroxisomes of etiolated seedlings (Supplemental Table S11; Supplemental Fig. S5). Among them were ICL and MLS, enzymes that operate strictly in the glyoxylate cycle (Eastmond et al., 2000; Cornah et al., 2004; Pracharoenwattana et al., 2005), small heat shock protein AtHsp15.7, ACETYL-COENZYME

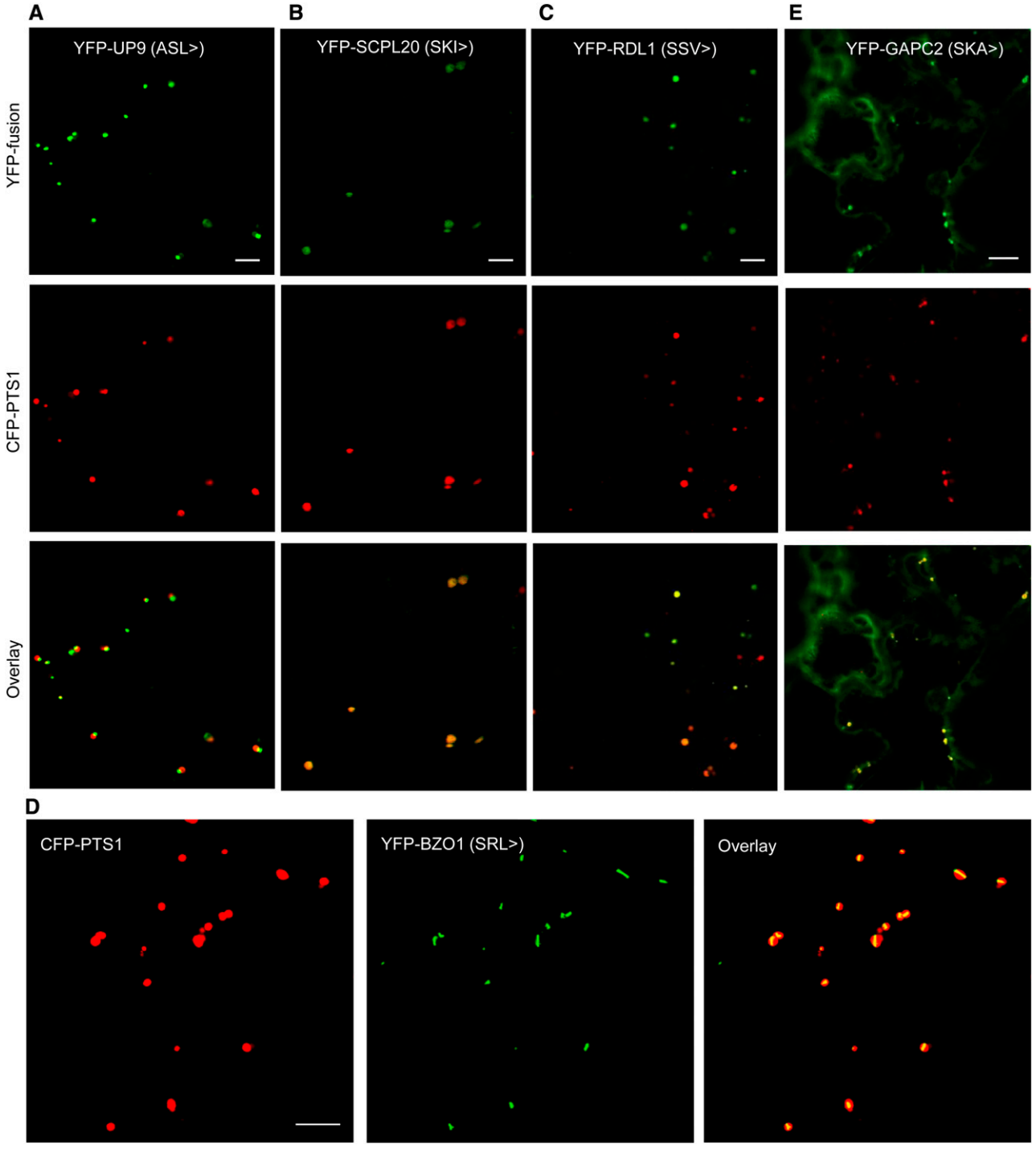


**Figure 3.** Peroxisomal localization validation. Shown are confocal microscopic images of leaf epidermal cells from 4-week-old tobacco plants coexpressing YFP fusions of the candidate proteins and the peroxisomal marker protein cyan fluorescent protein (CFP)-PTS1. Bars = 10 $\mu$m.

A THIOLASE1.3 (ACAT1.3), and the newly identified BZO1, RDL1, SCPL20, and UP9, suggesting that besides the glyoxylate cycle, there may also be a few biochemical processes more prevalent in seedling peroxisomes.

Peroxisomes in etiolated seedlings contained similar levels of core $\beta$-oxidation enzymes (Fig. 2, A and B) to those in leaf peroxisomes (Reumann et al., 2009), indicating that fatty acid $\beta$-oxidation is a major peroxisomal function throughout development. However,

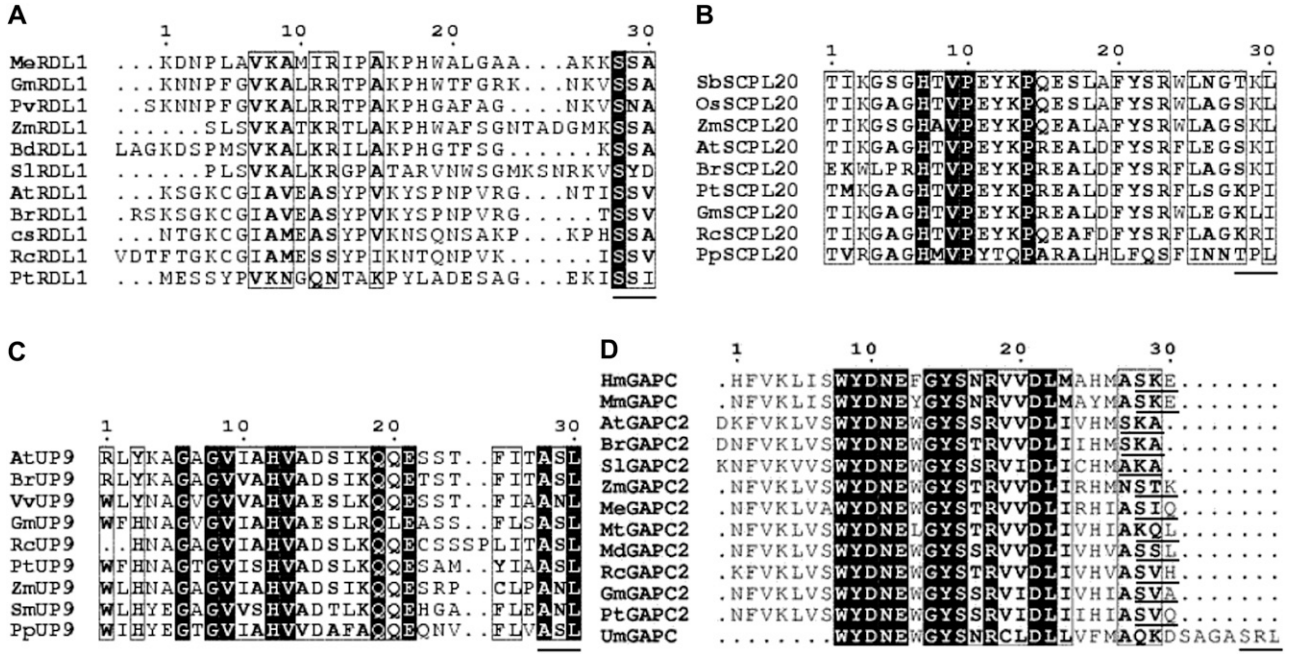


**Figure 4.** Alignment of C-terminal sequences of newly validated, plant-specific peroxisomal proteins and their homologs in other species. PTS1 or PTS-like tripeptide sequences are underlined. Abbreviations of species names are as follows: At, Arabidopsis; Bd, *Brachypodium distachyon*; Br, *Brassica rapa*; Cs, *Citrus sinensis*; Gm, soybean; Hs, *Homo sapiens*; Md, *Malus domestica*; Me, *Manihot esculenta*; Mm, *Mus musculus*; Mt, *Medicago truncatula*; Os, rice; Pp, *Physcomitrella patens*; Pt, *Populus trichocarpa*; Pv, *Phaseolus vulgaris*; Rc, *R. communis*; Sb, *Sorghum bicolor*; Sl, tomato; Sm, *Selaginella moellendorffii*; Um, *Ustilago maydis*; Vv, *Vitis vinifera*; Zm, maize.

some isoforms of $\beta$-oxidation enzymes found in leaf as well as cell culture peroxisomes were undetected in this study (Supplemental Table S11). For example, only four of the five functional ACX isoforms were detected. ACX5, the undetected isoform, is involved in wound-induced jasmonate biosynthesis (Schilmiller et al., 2007). In the case of thiolases, while KAT1 was only found in Z4, KAT2 was detected in all seven proteomics experiments, which is in agreement with previous studies that showed PED1/KAT2 to be the major form of 3-ketoacyl-CoA thiolase in seedlings (Hayashi et al., 1998; Germain et al., 2001). Enoyl-CoA isomerase, an important enzyme for the catabolism of unsaturated fatty acids with cis-double bonds at odd-numbered carbons (Goepfert et al., 2008), is the only other major core $\beta$-oxidation component that was undetected in etiolated seedling peroxisomes. Lastly, for AAEs and thioesterases, enzymes catalyzing reactions pertaining to the core peroxisomal $\beta$-oxidation pathway (Tilton et al., 2000; Shockey et al., 2003; Reumann et al., 2009), only three of the nine known AAEs and three of the six thioesterases were detected in our study, possibly due to the low abundance of the undetected isoforms or lack of their substrate(s).

Somewhat unexpectedly, except for SGT, we detected all the proteins implicated in peroxisomal steps of photorespiration (Table I), suggesting that peroxisomes of etiolated seedlings may have begun to accumulate photorespiratory enzymes even before light perception, or these enzymes have acquired nonphotorespiratory functions (see "Discussion").

Peroxisomes in etiolated seedlings house most of the known antioxidative enzymes (Table I). However, except for ASCORBATE PEROXIDASE3 (APX3), proteins of the peroxisomal ascorbate-glutathione detoxification system (Kaur et al., 2009), including the previously identified GR1, MDAR1 (Eubel et al., 2008; Reumann et al., 2009), and DHAR (Reumann et al., 2009), were not detected in this study. This suggests that catalase and copper/zinc superoxide dismutase may have more prominent roles in eliminating ROS species from seedling peroxisomes.

The five-member PEX11 family of peroxisome membrane proteins oversees the early steps of peroxisome division/proliferation (Lingard and Trelease, 2006; Orth et al., 2007). In contrast to leaf peroxisomes (Reumann et al., 2009), only three of the five members, PEX11a, PEX11d, and PEX11e, were detected in this study (Table I). PEX11b is induced by light (Desai and Hu, 2008); therefore, its absence in peroxisomes from dark-grown seedlings was not unexpected. However, we were intrigued by the lack of detection of PEX11c, especially since we found the less abundant isoform PEX11a (Orth et al., 2007) in this study. It has been speculated that the PEX11 isoforms have discrete roles in peroxisome multiplication (Hu, 2009); however, their functions have proven difficult to tease apart. Our data suggest that seedlings unexposed to light may mainly

use PEX11a, PEX11d, and PEX11e to promote peroxisome elongation.

### Expression Profiling of Genes Encoding Peroxisomal Proteins in Etiolated Seedlings

To determine whether genes encoding peroxisomal proteins of etiolated seedlings identified from this study confer any tissue-specific expression pattern, we queried the Botany Array Resource expression browser with all 77 genes (technically 76, as GOX1 and GOX2 shared the same probe), downloaded $\log_2$-normalized data for the relative expression of these genes from the AtGenExpress developmental time-line data set (Schmid et al., 2005; Toufighi et al., 2005; Supplemental Tables S12 and S13), and generated heat maps that clustered the peroxisomal genes based on their level of coexpression. Consistent with their established role in the postgermination process, genes encoding metabolic enzymes pertaining to $\beta$-oxidation and the glyoxylate cycle were strongly coexpressed in dry seeds and imbibed seeds. Conversely, photorespiratory enzyme genes appeared to be repressed at the same developmental stage. Hierarchical clustering also grouped genes encoding proteins in distinct biochemical processes, such as glyoxylate cycle, $\beta$-oxidation, and photorespiration, in discrete groups (Supplemental Fig. S6A). Focusing on 14 genes encoding proteins newly validated (Fig. 3; Supplemental Fig. S4) and proteins uniquely found in our study of etiolated seedlings (Supplemental Table S10), we found that, in line with their discovery in etiolated seedling peroxisomes, the genes for RDL1, SCPL20, BZO1, and UP9 were also highly expressed in dry seeds and imbibed seeds compared with other development time points or tissues (Fig. 5A). These results prompted us to examine the expression patterns of these genes during germination in more detail.

To dissect the expression profiles of genes encoding peroxisomal proteins in etiolated seedlings in the course of germination, we downloaded microarray data (GSE30223) from a recent study that carried out extensive transcriptional profiling of Arabidopsis seeds at crucial developmental intervals of the germination process (Narsai et al., 2011). All genes in this data set could be ordered into one of four distinct clusters of gene expression: cluster 1, genes steadily induced over the germination time course; cluster 2, stored transcripts highly expressed in the initial stages followed by a decline; cluster 3, genes exhibiting a characteristic expression spike toward the end of stratification that lasted only up to a period of 6 h of exposure to light; and cluster 4, genes with expression level unchanged during germination (Narsai et al., 2011). $\text{Log}_2$-normalized data were extracted for peroxisomal genes (Supplemental Table S14) to generate a heat map (Supplemental Fig. S6B).

The same 14 genes were analyzed, using *RPK1*, which was previously classified as a cluster 3 peroxisomal gene (Narsai et al., 2011), as a reference (Fig. 5B). *GAPC2*, *SCPL20*, and *RDL1* were cluster 1 genes, up-regulated

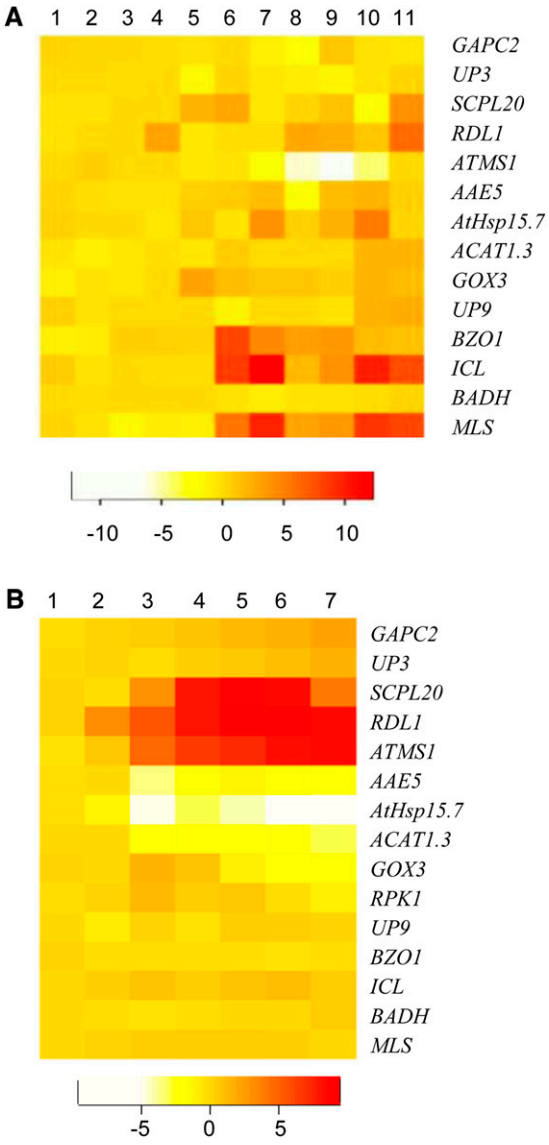


**Figure 5.** Heat maps showing relative expression levels of genes encoding a subset of peroxisomal proteins found in etiolated seedlings. A, $\text{Log}_2$-normalized expression at various developmental stages. Columns are as follows: 1, seedling cotyledons; 2, vegetative rosette; 3, flowering rosette; 4, flower stage 12; 5, senescing leaf; 6, seed 6 silique; 7, seed 10 silique; 8, embryo heart, cotyledon; 9, embryo torpedo, cotyledon; 10, dry seeds; 11, 24-h imbibed seed. B, $\text{Log}_2$-normalized expression during seed germination as compared with dry seed. Columns are as follows: 1, fresh seeds; 2, 12-h stratified seeds; 3, 48-h stratified seeds; 4, 6-h light-grown seeds; 5, 12-h light-grown seeds; 6, 24-h light-grown seeds; 7, 48-h light-grown seeds.

during germination and continuing to be so well into post germination. The transcript abundance of *AtHsp15.7* and *ACAT1.3* decreased in the germination/postgermination time period, indicating that they were cluster 2 genes. Similar to the cluster 3 gene *RPK1*, *GOX3* showed an expression peak followed by a decline. Akin to the marker genes *ICL* and *MLS*, the expression of *BZO1* and *UP9* did not appear to vary

greatly during germination, so they were considered cluster 4 genes (Fig. 5B).

In summary, the identification of some proteins only from this proteomic study of etiolated seedling peroxisomes seemed to be largely attributed to the much higher expression level of their genes in seeds.

### Mutant Analysis Revealed the Role for a Cys Protease in β-Oxidation and Development

To elucidate the functions of the newly validated peroxisomal proteins in plant development, we resorted to a reverse genetics approach by analyzing the transfer DNA (T-DNA) insertion mutants of these genes. We were able to obtain homozygous mutants for *BZO1*, *SCPL20*, *GOX3*, *GAPC2*, and *RDL1* (Fig. 6A). Reverse transcription (RT)-PCR analysis showed that while *bzo1-4*, *scpl20-1*, *gox3-1*, *gapc2-2*, and *rdl1-2* appeared to be null, *rdl1-1* retained partial expression of the gene, and interestingly, a T-DNA insertion in the 3′ untranslated region of the *SCPL20* gene in *scpl20-2* resulted in overexpression of the gene (Fig. 6B).

Given that β-oxidation of fatty acids is a major catabolic pathway contributing to gluconeogenesis during germination, mutants in β-oxidation components show compromised growth in the absence of exogenous Suc during early development (Hu et al., 2012). To test whether any of these newly validated peroxisomal proteins were involved in fatty acid β-oxidation, we measured the hypocotyl length of 7-d-old mutant seedlings grown in the dark on one-half-strength Linsmaier and Skoog (1/2 LS) medium with or without Suc. Although the control mutant *pex14*, which is defective in peroxisome matrix protein import (Hayashi et al., 2000), displayed strong Suc dependence, no obvious deficiencies were observed for any of the tested mutants (Supplemental Fig. S7A).

Since the conversion of IBA to indole-3-acetic acid also requires peroxisomal β-oxidation (Zolman et al., 2000), we checked if the mutants were disrupted in this aspect of peroxisome metabolism by measuring growth inhibition of primary root in response to IBA treatment. To this end, mutant seedlings were grown on 1/2 LS supplemented with different concentrations of IBA, and the length of primary root was measured after 7 d. Compared with wild-type plants, the two *rdl1* mutant alleles exhibited statistically significant resistance to 10 μM IBA (Fig. 7A), whereas the overexpression line *scpl20*-2 showed hypersensitivity to 10 μM IBA (Supplemental Fig. S7B). Based on these data, we predicted that both RDL1 and SCPL20 might play positive roles in peroxisomal β-oxidation.

We also examined if the functions of the identified proteins extended to photorespiration by comparing the growth of the mutants in ambient air versus low-$CO_2$ (80 μL $L^{-1}$) conditions. Only *rdl1-2* exhibited noticeable differences in appearance under low $CO_2$ by showing strong growth inhibition, and this phenotype could not be rescued by elevated $CO_2$ (1,000 μL $L^{-1}$),

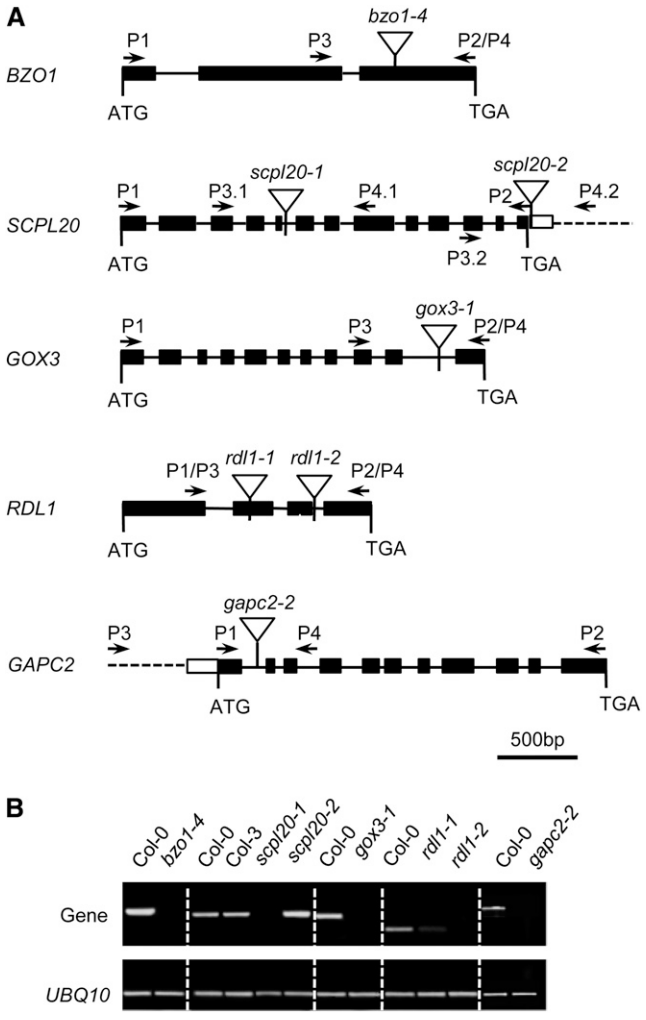


**Figure 6.** Identification of T-DNA insertion mutants of newly validated peroxisomal genes. A, Gene structures. Black boxes, Coding regions; white boxes, untranslated regions; solid lines, introns; dashed lines, intergenic regions; triangles, positions of the T-DNA insertions. Primers used for genotyping and RT-PCR are also indicated. B, RT-PCR analysis of RNA from 7-d-old seedlings. PCR products amplified from *UBQ10* are loading controls.

under which conditions *rdl1-2* plants were still small and had chlorotic and faster senescing leaves (Fig. 7B). Thus, these peroxisomal proteins do not seem to play strong roles in photorespiration, and RDL1 appears to be involved in nonphotorespiratory processes that impact plant growth under stress conditions.

It has been proposed that peroxisomal metabolic pathways are an important determinant of germination potential and postgerminative seedling growth (Footitt et al., 2006; Hu et al., 2012). Considering the detection of these new proteins in seedling peroxisomes and the strong expression for some of them during seed germination, we investigated their roles in germination. Since fresh seeds from all the mutants germinated normally on regular medium, we quantified radicle emergence from the seeds in the presence

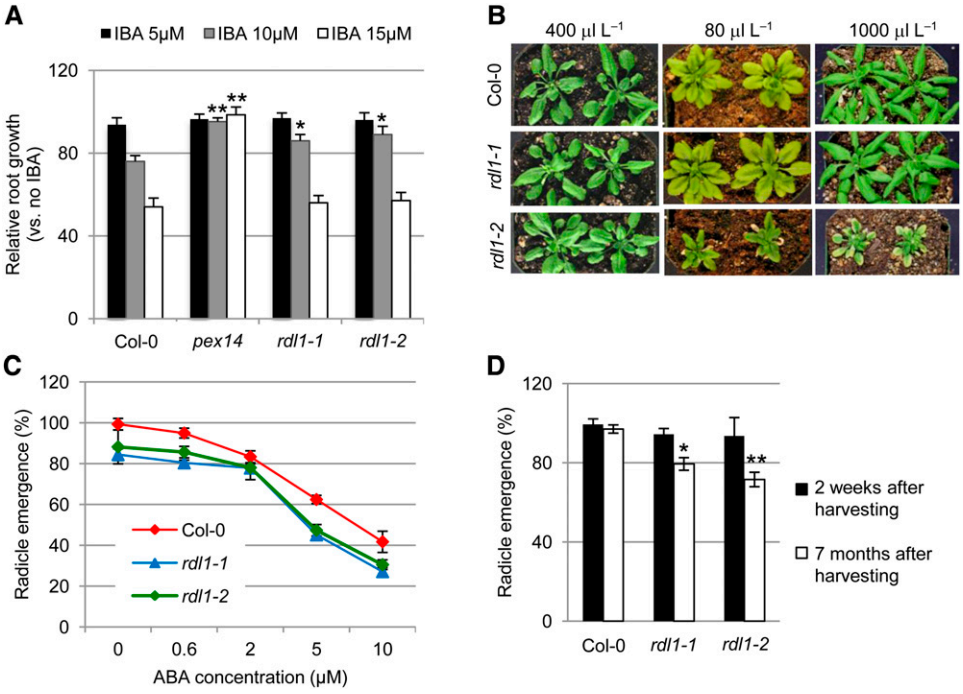


**Figure 7.** Phenotypic analysis of the *rdl1* mutants. A, IBA response assays. Relative root lengths (on IBA versus without IBA) of 7-d-old seedlings on 1/2 LS medium supplemented with 5, 10, or 15 $\mu$M IBA are shown. Data represent means ±SE of three independent experiments. For each experiment, $n = 50$. Asterisks indicate changes significantly different from that in the wild type (Col-0, Columbia; Student's *t* test: $^*P < 0.05$, $^{**}P < 0.005$). B, Images of 4-week-old plants grown in ambient air (400 $\mu$L $L^{-1}$ $CO_2$) or under low (80 $\mu$L $L^{-1}$) or high (1,000 $\mu$L $L^{-1}$) $CO_2$. C and D, Seed germination assays. Percentage of radicle emergence from seeds 6 d after growing on Linsmaier and Skoog medium (C) or Linsmaier and Skoog medium supplemented with the indicated concentrations of ABA (D) was quantified. Each data point represents the mean ± SE of three independent experiments ($n = 100$ per experiment). For Student's *t* test in C, $P < 0.005$. In D, asterisks indicate changes significantly different from that in the wild type (Student's *t* test: $^*P < 0.05$, $^{**}P < 0.005$).

of the phytohormone abscisic acid (ABA), a known inducer of seed dormancy and inhibitor of germination. Like the wild type, *bzo1-4*, *scpl20-1*, *scpl20-2*, *gapc2-2*, and *gox3-1* showed steadily decreased radicle emergence with increased concentrations of ABA (Supplemental Fig. S7C). However, both *rdl1-1* and *rdl1-2* were partially hypersensitive to ABA (Fig. 7C), indicating that RDL1 possibly represses the ABA response pathway in seed germination. Interestingly, after prolonged storage, the germination rate of the *rdl1* mutant seeds dropped significantly in comparison with wild-type plants and other mutants. Within 7 months of seed harvesting, seed germination rate decreased approximately 20% in the knockdown allele *rdl1-1* and approximately 30% in the null allele *rdl1-2* (Fig. 7D), supporting a role for RDL1 in seed viability.

## DISCUSSION

### A Road Map of the Peroxisomal Proteome in Etiolated Arabidopsis Seedlings

Proteome analyses of the Arabidopsis leaf peroxisomes provided a comprehensive understanding of the metabolic pathways occurring in peroxisomes of photosynthetic tissues (Reumann et al., 2007, 2009). However, what exactly occurs inside another major plant peroxisomal variant (i.e. those in seeds and dark-grown seedlings) remained poorly understood. This work has presented a much-needed comprehensive view of the metabolic pathways in peroxisomes in dark-grown seedlings. We demonstrated that the proteomes of the two dominant peroxisomal subtypes in Arabidopsis overlap significantly, differing mainly in the use of isozymes. In addition to proteins in the glyoxylate cycle, this study also revealed and later confirmed the existence of previously unknown peroxisomal proteins that would suggest tissue-specific peroxisomal functions (see below).

Although the detection of photorespiratory enzymes in etiolated seedlings was somewhat surprising, a previous analysis of peroxisomes from 7-d-old etiolated soybean seedlings found some of the photorespiratory enzymes as well (Arai et al., 2008a), and immunoblot of the dark-grown soybean tissue detected the GOX protein (Arai et al., 2008b). These data suggest that peroxisomes may have begun to accumulate enzymes involved in photorespiration even without perceiving light. This is similar to the observed abundant presence of Rubisco and several other proteins that function in photosynthesis in the rice (*Oryza sativa*) etioplast proteome

(von Zychlinski et al., 2005; Kleffmann et al., 2007). An alternative explanation would entail the functional diversification of these enzymes to acquire nonphotorespiratory functions. Although roles in pathogen defense have been reported for Arabidopsis GOX (Rojas et al., 2012), melon (*Cucumis melo*) SGT (Taler et al., 2004), and soybean HPR (Okinaka et al., 2002), their roles in etiolated tissues remain unclear.

The use of duplicate experiments on total peroxisomes and ZOOM fractionation prior to 1-DE allowed us to enhance the dynamic range of protein detection and provided a significant improvement over previous proteomic studies conducted on similar tissue. However, the low tissue yields of dark-grown Arabidopsis seedlings added a level of difficulty to isolate large amounts of highly pure peroxisomes for membrane enrichment. Thus, despite the identification of 77 proteins, we were still unable to detect many membrane proteins known to be involved in peroxisome biogenesis, a persistent problem in plant membrane peroxisome proteomics investigations to date. Therefore, improvements need to be made in the choice of species (preferably oilseed species with large seeds and seedlings) and in isolation procedures to identify peroxisomal membrane proteins.

Although the vast majority of the proteins are conserved in the peroxisomal proteome of leaf, cell culture, and etiolated seedlings, it is worth noting that some differences also exist. This is unlike mammalian peroxisome proteomics studies, where only one protein was found to vary between liver and kidney tissues (Kikuchi et al., 2004; Ofman et al., 2006; Islinger et al., 2007). In the case of plants, it is also apparent that physiology is an important determinant of the nature of peroxisomal proteins that are found or missing, as the case may be. For instance, all 16 proteins undetected in cell cultures but found in etiolated seedlings share high expression in seeds/imbibed seeds (Supplemental Fig. S6A). One of these genes encodes a small heat shock protein, AtHsp15.7, a previously characterized peroxisome matrix protein (Ma et al., 2006) that could not be detected in Arabidopsis leaf peroxisomes. Likewise, eight proteins that are found only in leaf peroxisomes are encoded by light-inducible genes (Peschke and Kretsch, 2011). Furthermore, enzymes belonging to protein families seem to utilize specific isoforms in different tissues; thus, proteomic studies enable the dissection of functional roles of such isozymes. Finally, for many proteins, it is likely that variations in different tissues are more quantitative than qualitative in nature, a hypothesis that requires further testing in the future by analyzing plant peroxisome proteome dynamics.

The peroxisomal localization of ATMS1 and GAPC2 suggests that SAK> and SKA> may be new PTS1 sequences. In contrast, despite possessing a major C-terminal PTS1, one of the candidate proteins (GSA2, SRL>) did not localize to peroxisomes, possibly because the targeting signal was not surface exposed. Other candidate proteins that contain weak PTS1s (LKL>) or PTS1-like tripeptides (AKA>, GKL>, MLL>) did not localize to peroxisomes either (Supplemental Table S9). Peroxisome prediction algorithms have been refined by incorporating information from upstream enhancer sequences (Lingner et al., 2011); thus, proteins that failed to localize to peroxisomes can now be used as a false positive data set to improve prediction algorithms. Moreover, we cannot rule out the possibility that several candidate proteins that failed to localize to peroxisomes in our hands are subject to other means of peroxisome targeting via "piggybacking" or the use of regulatory strategies that result in differential compartmentalization of proteins. Plant peroxisomal proteins such as KAT5, transthyretin-like protein, soybean Asp aminotransferase, and enzymes of the isoprenoid pathway employ such transcriptional and translational variants for localization (Gebhardt et al., 1998; Carrie et al., 2007; Reumann et al., 2007; Sapir-Mir et al., 2008; Lamberto et al., 2010; Thabet et al., 2011). Additionally, some proteins may use internal signals to direct proteins to peroxisomes, which may have been occluded in our fluorescent protein fusion constructs, accounting for the lack of peroxisomal localization in our transient assays.

### Revelation of Peroxisomal Proteolysis in Etiolated Seedlings

Seed germination is defined by rapid surges in the plant's transcription and translation circuitry as it gears toward the switch from a heterotrophic to an autotrophic mode of life (Weitbrecht et al., 2011). This transition also affects peroxisomes, which similarly need to rewire their metabolism by proteome remodeling, possibly through importing new proteins or degrading superfluous proteins. Two peroxisomal proteases had been characterized in Arabidopsis, both of which are conserved in eukaryotes. DEG15 is a trypsin-like Ser protease that cleaves the N-terminal sequence from PTS2-containing proteins (Helm et al., 2007; Schuhmann et al., 2008). LON2 is a member of the AAA ATPase superfamily that has been detected in both leaf (Reumann et al., 2009) and etiolated seedling (this study) peroxisomes. Its absence from plants resulted in retarded plant growth due to a deleterious effect on the import of matrix proteins (Lingard and Bartel, 2009).

Germination is a complex process that can be divided into three phases: (1) rapid imbibition of water by the dry seed, (2) relatively limited water uptake, and (3) an increase of water uptake followed by radicle emergence from the seed (Weitbrecht et al., 2011). RDL1 belongs to the plant papain-like Cys protease subfamily 1 that contains eight other members, including RD21A (Richau et al., 2012). A Daikon radish (*Raphanus sativus*) homolog of RDL1 has Cys protease activity and is exclusively expressed during early phases of germination (Tsuji et al., 2013). Similarly, the expression of Arabidopsis *RDL1* remains relatively low in dry seed but is rapidly induced in response to seed imbibition and steadily increases until it reaches a peak toward the end

of the germination period (Fig. 5). Both *rdl1* mutant alleles are resistant to 10 $\mu$M IBA and hyperresponsive to ABA-mediated inhibition of seed germination, and seeds of the null *rdl1* allele lose vigor in an age-dependent manner (Fig. 7, A, C, and D). IBA resistance and reduced seed germination phenotypes are also associated with a plethora of mutants in the peroxisomal $\beta$-oxidation pathway (Russell et al., 2000; Zolman et al., 2001; Pinfield-Wells et al., 2005; Pracharoenwattana et al., 2005; Kanai et al., 2010). Together, these results led us to conclude that RDL1 may impact peroxisomal $\beta$-oxidation-related pathways in seed germination. In addition, *rdl1-2*'s increased vulnerability to both low- and high-$CO_2$ conditions (Fig. 7B) indicates that RDL1 may be crucial to the stress response. This is similar to the reported role of Arabidopsis RD21A, an ortholog of tomato (*Solanum lycopersicum*) immune protease C14, in plant immune response (Shindo et al., 2012). The identification of substrates for RDL1 may shed light on its role in peroxisomal metabolism and disparate physiological processes pivotal to seed vigor and stress adaptation.

Serine carboxypeptidase-like (SCPL) proteins are annotated as peptidases but have diversified in plants to include acyltransferase, lyase, and esterase activities involved in the production of an array of secondary metabolites (Fraser et al., 2005; Gershater et al., 2007; Clauss et al., 2008; Vlot et al., 2008). SCPL20 is one of the two members of clade IB of the SCPL family, with conserved catalytic triad and carboxylate-binding residues (Fraser et al., 2005). Activity-based protein profiling coupled with Multidimensional Protein Identification Technology (MudPIT) analysis established SCPL20 as a Ser hydrolase (Kaschani et al., 2009). The overexpression allele of *SCPL20* is hypersensitive to 10 $\mu$M IBA (Supplemental Fig. S7B), indicating that SCLP20 may facilitate $\beta$-oxidation, a hypothesis that needs to be further tested with additional genetic and biochemical analyses. SCPL20 was also detected in the apoplast proteome in response to *Verticillium longisporum* infection, suggesting that it might play a role in plant defense (Floerl et al., 2012). Given the wide spectrum of activities associated with SCPLs, a more detailed characterization is needed to establish whether SCPL20 is involved in degradation, metabolism, or defense. In light of the recent finding that SCPLs carry out benzoylation and sinapoylation of glucosinolate side group R (Lee et al., 2012), it would be particularly interesting to examine the glucosinolate profile of the *scpl20* alleles.

### BA Biosynthesis in the Peroxisome

BA is the precursor for the synthesis of a variety of phytochemicals, including salicylic acid and aromatic volatiles, which play diverse roles in plant metabolism and defense (Wildermuth, 2006). BA biosynthesis is proposed to occur via several alternate routes; one branch is known to utilize the peroxisomal $\beta$-oxidation pathway to produce BA from cinnamic acid (Beuerle and Pichersky, 2002). Reducing the expression of any of the petunia enzymes catalyzing successive steps of this $\beta$-oxidative pathway led to profoundly compromised emission of benzenoid volatiles, providing conclusive evidence for BA synthesis in peroxisomes (Van Moerkercke et al., 2009; Colquhoun et al., 2012; Klempien et al., 2012; Qualley et al., 2012). Peroxisomal enzymes responsible for this conversion were identified as the acyl-activating enzymes PhCNL and PhAAE, followed by cinnamoyl CoA hydratase/dehydrogenase and PhKAT (Van Moerkercke et al., 2009; Colquhoun et al., 2012; Klempien et al., 2012; Qualley et al., 2012).

BZO1, the Arabidopsis homolog of PhCNL, was initially identified from a forward genetic screen conducted on seeds for altered accumulation of benzoylglucosinolates (Kliebenstein et al., 2007). A more recent study confirmed that, akin to PhCNL, BZO1 acts in the first committed step of peroxisomal BA biosynthesis (Lee et al., 2012). It is worth noting that, unlike in petunia, the highest level of benzoylglucosinolates is found in seeds in Arabidopsis (Petersen et al., 2002; Brown et al., 2003). Thus, it is not surprising that we found BZO1 only in proteomics of etiolated seedling peroxisomes. BZO1 exhibits a somewhat unusual ring-like localization pattern on the peroxisome (Fig. 3D); whether there is any biological significance to this phenomenon awaits further investigation. BZO1 belongs to the plant-specific clade of the acyl-activating enzyme superfamily, of which several members (e.g. close homologs AAE11 and AAE12) contain PTS1 (Shockey et al., 2003). Although AAE11 shares high sequence similarity with PhAAE, it is unknown whether AAE11 or AAE12 also acts in BA biosynthesis.

CHY1 is another peroxisomal protein implicated in BA synthesis, although its exact mode of action has not been resolved (Ibdah and Pichersky, 2009). The identity of Arabidopsis peroxisome proteins corresponding to PhCNL and PhKAT is still unclear. However, considering the gene expression profile, sequence similarity, and the suggestion that developing seeds synthesize BA exclusively through the peroxisomal pathway, AIM1 and KAT5 appear to be likely candidates playing equivalent roles to PhCNL and PhKAT. Furthermore, based on enzyme activity and coexpression with BZO1, 1,4-DIHYDROXY-2-NAPHTHOATE-COENZYME A THIOESTERASE2 seems likely to oversee the conversion of BA-CoA to BA in peroxisomes (Widhalm et al., 2012). Finally, recent works have credited a suite of peroxisomal proteins with roles in immune responses (Taler et al., 2004; Lipka et al., 2005; Bednarek et al., 2009; Clay et al., 2009; Coca and San Segundo, 2010; Li et al., 2012; Rojas et al., 2012). Given that BA derivatives such as salicylic acid, benzoylglucosinolates, and phytoalexins are important for plant defense, it will be interesting to explore the roles of the peroxisomal BA biosynthetic proteins in defense-related functions.

### Dual-Localized GAPC2

GAPCs are ubiquitous enzymes of the glycolytic pathway, phosphorylating glyceraldehyde-3-phosphate

to convert it to 1,3-bisphosphoglycerate. GAPC in mammals also performs nonmetabolic functions in processes such as apoptosis, vesicular transport, DNA repair and replication, transcription, and tRNA export (Sirover, 2011; Tristan et al., 2011). These functions are partially achieved via posttranslational modifications of the substrate enzyme following oxidative stress to affect the localization and function of the enzyme. Arabidopsis possesses seven GAPCs, of which GAPC1 and GAPC2 were found in the cytosol and the remaining five in the plastid (Rius et al., 2006; Muñoz-Bertomeu et al., 2009). GAPC1 and GAPC2 have also been attributed nontraditional roles as oxidative stress sensors that bind phospholipase D to transduce hydrogen peroxide signals, thereby activating plant stress responses (Guo et al., 2012).

GAPC2 protein isoforms in several fungal species are peroxisomal as a consequence of alternative splicing or translational read-through events (Freitag et al., 2012). We have shown that at least a fraction of GAPC2 goes to peroxisomes (Fig. 3E). It should be noted that previous reports on GAPC2's localization had YFP fused to the C terminus of the protein, which would mask PTS1 (Guo et al., 2012; Vescovi et al., 2013). Since NADH is a by-product of GAPC reaction, we speculate that GAPC2 may play an auxiliary role in augmenting the peroxisomal pool of reduced cofactor.

### UP9, a Peroxisomal Lipase?

YFP-UP9 only partially overlaps with the peroxisomal marker, which is reminiscent of the peripheral peroxisome association exhibited by SNOWY COTYLEDON3 (SCO3; Albrecht et al., 2010). These proteins carry matrix-targeting signals (UP9, ASL>; SCO3, SRL>) but appear to be associated with the surface of the organelle, suggesting that the mechanics of peroxisome protein import and targeting are very complex and our knowledge of the mechanics is far from complete. Although UP9's function is unknown, this protein contains an $\alpha/\beta$-hydrolase fold typically found in lipases (Hunter et al., 2012). Peroxisomal lipases exist in both yeast (Thoms et al., 2008) and mammals (Yang et al., 2003). Interestingly, the intracellular localization of mammalian phospholipase A2$\gamma$ is dynamically regulated at both transcriptional and translational levels, which determine whether the protein localizes to peroxisomes or mitochondria or both (Mancuso et al., 2004). Information from The Arabidopsis Information Resource database (www.arabidopsis.org) indicates that UP9 also has two other alternative protein-coding isoforms, neither of which terminates in a PTS1, suggesting that, like mammalian phospholipase A2$\gamma$, the protein targeting of UP9 may be regulated at the transcriptional level. The localization pattern, protein domain assignment, and relatively high expression in seeds (Fig. 5), a developmental time frame that strongly coincides with lipid mobilization, suggest that UP9 is likely a peroxisome membrane-associated lipase.

## CONCLUSION

In this study, we provide a comprehensive atlas of the peroxisomal proteome in etiolated seedlings. The identification of 77 peroxisomal proteins from this tissue enabled us to compare the metabolic pathways in the two major plant peroxisomal variants, which turned out to be largely overlapping. Mutant analysis discovered the involvement of the RDL1 Cys protease in $\beta$-oxidation and development. In summary, this study revealed common functions of peroxisomes in dark-grown seedlings and green leaves and uncovered activities highly expressed in peroxisomes of dark-grown seedlings, providing the basis for future investigations of peroxisomal proteolytic processes and their contribution to germination and postgerminative growth.

A recent in silico analysis of the Arabidopsis genome predicted the number of plant peroxisomal proteins to possibly exceed 400 (Lingner et al., 2011). To understand the full spectrum of peroxisomal functions and the dynamics of the peroxisomal proteome, new technologies will be needed to uncover low-abundance proteins and transient proteins that are only present in specific tissues/cell types or in response to certain environmental cues. A complete understanding of the metabolic capabilities of various peroxisomal variants and their regulation in plants will be instrumental to studies aimed at rational engineering of peroxisome-related processes, such as photorespiration and lipid metabolism, to improve biomass production. To this end, proteomics should be combined with other large-scale approaches such as transcriptomics and metabolomics. Finally, technologies employed in the reference plant Arabidopsis may also be applied to the study of crop species, such as rice, which was predicted to contain a conserved peroxisomal proteome with Arabidopsis (Kaur and Hu, 2011), and other economically important plants.

## MATERIALS AND METHODS

### Plant Materials and Growth Conditions

Arabidopsis (*Arabidopsis thaliana*) ecotype Columbia was used for peroxisome isolation. A piece of autoclaved Whatman paper was placed on top of an autoclaved WypAll wipe (Kimberly-Clark; for absorbing water) at the bottom of a 150- × 15-mm petri dish and soaked with autoclaved deionized water. Seeds were surface sterilized and evenly spread on the Whatman paper. The petri dish was then sealed with a Parafilm membrane and wrapped in aluminum foil. After 2 d of stratification at 4°C, petri dishes were exposed to light for 1 h to synchronize germination, rewrapped in foil, and placed in a Percival growth chamber at 22°C. Three days later, germinated seedlings were used for peroxisome isolation.

For other assays, Columbia-0 and Columbia-3 were used as controls. Mutants obtained from the Arabidopsis Biological Resource Center and the Nottingham Arabidopsis Stock Centre include *scpl20-1* (SAIL_392C07), *scpl20-2* (SALK_147839), *gox3-1* (SALK_020909), *rdl1-1* (SALK_085378), *rdl1-2* (SALK_051510), and *gapc2-2* (SALK_070902). The T-DNA insertion mutant line *bzo1-4* (SALK_094196; Kliebenstein et al., 2007) was obtained from Dr. Clint Chapple. Seeds were surface sterilized and plated on 1/2 LS medium (Caisson Laboratories) solidified with 1% (w/v) agar and supplemented with Suc or hormones, as indicated. Plants were grown at 22°C under continuous illumination at 75 $\mu$mol photons $m^{-2}$ $s^{-1}$ or darkness. Homozygous lines were identified by PCR screening using genomic DNA from seedlings.

## Isolation of Peroxisomes and Protein Separation

Approximately 25 g of 3-d-old etiolated seedlings (from approximately eight petri dishes of approximately 3 g of seeds) was used for each peroxisome isolation, using procedures modified from the protocol described by Reumann et al. (2007). Seedlings were scraped off in complete darkness from the Whatman papers and kept in darkness until grinding buffer was added to the sample in the mortar, after which the procedure was performed under light. Samples were homogenized using a mortar and pestle in grinding buffer that contained 0.17 M Tricine-KOH (pH 7.5), 0.5 M Suc (17.1 g per 100 mL), 2% (w/v) bovine serum albumin, 2 mM EDTA, 5 mM dithiothreitol (0.0385 g per 100 mL), 10 mM KCl, 1 mM $MgCl_2$, 0.5% (w/v) polyvinylpyrrolidone-40, 0.1 mM phenylmethylsulfonyl fluoride, and protease inhibitor cocktail containing 0.2 mM $\varepsilon$-amino carproic acid, 0.2 mM benzamide, and 1 $\mu$g $mL^{-1}$ aprotinin, leupeptin, and peptatin. The homogenized sample was filtered through two-layer Miracloth to obtain crude extract and centrifuged at 7,000 rpm (SS34 rotor on a Sorvall RC 5C plus) at 4°C for 5 min to remove most chloroplasts. After discarding the pellet, the supernatant was loaded onto the top of a Percoll density gradient prepared in TE buffer (20 mM Tricine-KOH, pH 7.5, and 1 mM EDTA; gradient from bottom to top: 3 mL of 25% [w/v] Suc, 3 mL of 1:1 mixture of 25% [w/v] Suc and 32% [v/v] Percoll, 10 mL of 32% [v/v] Percoll, and 3 mL of 15% [v/v] Percoll) and centrifuged at 10,500 rpm for 15 min and then at 15,000 rpm (SS34 rotor) for 20 min at 4°C. Most of the supernatant was removed, leaving 2 to 3 mL at the bottom of the tube for pellet resuspension. The resuspended pellet was then washed with 2 volumes of 25% (w/v) Suc in TE buffer (added slowly), followed by centrifugation at 18,000 rpm for 30 min. The pellet was gently homogenized and loaded on top of a discontinuous Suc density gradient prepared in TE (bottom to top: 1 mL of 60% [w/v] Suc, 1 mL of 55% [w/v] Suc, 0.5 mL of 51% [w/v] Suc, 2 mL of 49% [w/v] Suc, and 1 mL of 46% [w/v] Suc, 44% [w/v] Suc, 41% [w/v] Suc, and 36% [w/v] Suc) and then ultracentrifuged for 30 min at 25,000 rpm (Beckman SW40 Ti). A milky band in the 51% Suc, which contained highly enriched and intact peroxisomes, was the target fraction and was carefully harvested with a pipetman or glass pipette. Typically, approximately 200 to 300 $\mu$g of peroxisomes was obtained from approximately 25 g of starting material, as determined by the Lowry method of protein estimation (Lowry et al., 1951).

To get peroxisomal membranes, isolated peroxisomes were diluted in 4 volumes of TE buffer and centrifuged at 50,000*g*. The pellet was washed in 100 mM $Na_2CO_3$ and then centrifuged at 100,000*g*. The pellet, which contains integral membrane proteins, was dissolved in SDS-PAGE loading buffer and used for 1-DE LC-MS/MS.

A ZOOM IEF Fractionator (Invitrogen) was used to separate peroxisomal proteins by pI. We used the standard configuration, which covers a pH range of 3.0 to 10.0. Total proteins were separated into five groups with the following pI ranges: 3.0 to 4.6, 4.6 to 5.4, 5.4 to 6.2, 6.2 to 7.0, and 7.0 to 10.0. Proteins in each subgroup were then subjected to 1-DE LC-MS/MS for protein identification. Due to the low amount of proteins in fractions with pH 4.6 to 5.4 and 5.4 to 6.2, gels from these two fractions were combined for mass spectrometry analysis.

## Immunoblot Analysis

For immunoblot analysis of samples from density gradients, the Percoll gradient was divided into 14 fractions (2 mL per fraction) and the Suc gradient was divided into 11 fractions (1 mL per fraction) from the top to the bottom of the tube. After collection, each fraction was briefly centrifuged, and the supernatant from each fraction was mixed with 4 volumes of SDS buffer and subjected to electrophoresis using a 10% (w/v) SDS-PAGE gel. After proteins were transferred to polyvinylidene difluoride membranes (Millipore), the membranes were blocked with 4% (w/v) nonfat dry milk dissolved in 1× Tris-buffered saline buffer and incubated for 1 h at room temperature with the following primary antibodies for western analysis: TIC110 (1:5,000, rabbit), PEX14 (1:2,500, rabbit), and VDAC (1:2,500; mouse).

## Mass Spectrometry Analysis and Peptide Identification

After 1-DE, each gel lane was cut into slices, which were digested by trypsin before LC-MS/MS using an LTQ-FTICR mass spectrometer (ThermoFisher) as described previously (Reumann et al., 2009). Tandem mass spectra were converted to peak lists by BioWorks browser version 3.2 (ThermoFisher) software with default parameters and analyzed using Mascot version 2.2 (Matrix Science). Mascot was set up to search The Arabidopsis Information Resource 9 database (20090619 version; 33,410 entries) assuming that the digestion enzyme was nonspecific. Mascot was searched with a fragment ion mass tolerance of 0.80 D and a parent ion tolerance of 10.0 $\mu$L $L^{-1}$. The iodoacetamide derivative of Cys was specified in Mascot as a fixed modification. Oxidation of Met was specified in Mascot as a variable modification.

Scaffold (version Scaffold_3_00_03; Proteome Software) was used to validate tandem mass spectrometry (MS/MS)-based peptide and protein identifications. Peptide identifications were accepted if they could be established at greater than 50.0% probability as specified by the Peptide Prophet algorithm (Keller et al., 2002). Protein identifications were accepted if they could be established at greater than 99.0% probability and contained at least one identified peptide. Protein probabilities were assigned by the Protein Prophet algorithm (Nesvizhskii et al., 2003). Proteins that contained similar peptides and could not be differentiated based on MS/MS analysis alone were grouped to satisfy the principles of parsimony. Reverse directory matches were manually removed. QV, number of assigned spectra, number of unique peptides, number of unique spectra, percentage coverage, percentage of total spectra, and protein identification probabilities were exported from Scaffold version 3.00.3 after selecting the Biological Sample view for each of the seven proteomics experiments. False discovery rates reported are as determined by Scaffold version 3.00.3 with the specified settings (99% confidence for protein identification with a minimum of one peptide detected with 50% confidence for peptide identification). For proteins with single peptide identifications (only found in Z4), MS/MS spectra were manually screened and Mascot ion scores were inspected (cutoff of 30) prior to inclusion of the known peroxisomal proteins (MS/MS spectra for these known peroxisomal proteins are shown in Supplemental Document S1) on our list.

The Arabidopsis Subcellular Database SUBA3 (Tanz et al., 2013) was queried to retrieve information about the subcellular localization for all proteins identified in the respective experiments. We also compared the identified proteins with a list of known peroxisomal proteins (Kaur and Hu, 2011) to assign proteins unambiguously to the peroxisome. Proteins newly validated to be peroxisomal in this study were later included in this list. QV (exported from Scaffold 3.00.3) were totaled for the proteins assigned to each subcellular compartment ($QV_{Compartment}$) and compared with QV for all proteins identified ($QV_{All}$) in the experiment. Percentage distribution of proteins was calculated as $(QV_{Compartment}/QV_{All}) \times 100$.

## Measurement of ICL Activity

ICL catalyzes the hydrolysis of isocitrate into glyoxylate and succinate, and its activity was measured as described previously (Dixon and Kornberg, 1959) using cell extracts from germinated seedlings or various fractions collected from the peroxisome isolation process.

## In Vivo Targeting Analysis of YFP-Tagged Proteins

We used the Gateway cloning vectors developed for the leaf peroxisome study (Reumann et al., 2009) to clone candidate genes as either N- or C-terminal YFP fusion proteins. Primer sequences used for cloning are listed in Supplemental Table S15. Agroinfiltration and confocal laser scanning microscopy of tobacco (*Nicotiana tabacum*) leaf epidermal cells transiently expressing the tested proteins were performed as described by Reumann et al. (2009). Localization results for all clones tested are listed in Supplemental Table S9.

## Microarray Analysis

For expression at various developmental stages, $log_2$-normalized data for the relative expression were obtained from the Botany Array Resource expression browser (Schmid et al., 2005; Toufighi et al., 2005) and are listed in Supplemental Table S12. Details of the AtGenExpress developmental time-line data set used (Schmid et al., 2005; Toufighi et al., 2005) are listed in Supplemental Table S13. For expression in the course of germination, CEL files were downloaded from the Gene Expression Omnibus data set GSE30223 from the National Center for Biotechnology Information database. $Log_2$-normalized values for peroxisomal genes were extracted (Supplemental Table S14). Heat-map and clustering analyses were carried out as described previously (Kaur et al., 2013).

## RNA Analysis

Plants were grown for 7 d on medium with 1% (w/v) Suc, and total RNA was isolated from seedlings as described previously (Mallory et al., 2001). After treating with DNaseI (Qiagen), 1 $\mu$g of each RNA sample was reverse

transcribed using the iScript cDNA Synthesis kit (Bio-Rad). PCR amplification using 50 ng of complementary DNA was performed for 25 (for UBQ10) or 35 (for tested genes) cycles. The gene-specific primers used for RT-PCR and genotyping are summarized in Supplemental Table S16.

## Physiological Assays

For germination assays, seeds were plated on Linsmaier and Skoog medium supplemented with or without ABA (Sigma-Aldrich), stratified at 4°C for 4 d, and grown in Percival growth chambers. After day 6, radicle emergence was scored. All the data are representative of at least three independent experiments. For each experiment, $n = 100$.

For Suc dependence analysis, seeds were placed on plates supplemented with or without 1% (w/v) Suc and stratified at 4°C for 2 d. Hypocotyls were measured on 7-d-old seedlings grown in the dark. To study the IBA response, seeds were sown on plates containing 0.5% (w/v) Suc and IBA (Sigma-Aldrich) and stratified at 4°C for 2 d before the plates were placed in a growth chamber with continuous low-intensity light for 7 d. Hypocotyls were scanned using an EPSON scanner (Epson Perfection 4870 PHOTO) and measured using ImageJ version 1.43u. All the data are representative of at least three independent experiments. For each experiment, $n = 50$.

To observe photorespiratory phenotypes, 2-week-old seedlings were transferred from plates to soil and placed in a controlled-environment growth cabinet with light intensity of 115 $\mu$mol photons $m^{-2}$ $s^{-1}$, 20°C, a 16-h/8-h photoperiod, and $CO_2$ concentration of 80, 400 (ambient air), or 1,000 $\mu$L $L^{-1}$. Plants were photographed with a COOLPIX 8800 VR camera (Nikon).

Accession numbers of all the proteins described in this study can be found in Table I. Sequences used for alignment in Figure 4 are shown in Supplemental Document S2.

## Supplemental Data

The following materials are available in the online version of this article.

**Supplemental Figure S1.** ICL activity of Arabidopsis seedlings after growing 3 to 6 d.

**Supplemental Figure S2.** Silver-stained gel for the immunoblot shown in Figure 1D.

**Supplemental Figure S3.** Subcellular distribution of proteins identified from total peroxisomes (T1 and T2) in this study based on protein number.

**Supplemental Figure S4.** Verification of peroxisomal localization for six proteins identified from this study and our previous leaf peroxisomal proteomics but not confirmed before.

**Supplemental Figure S5.** Comparison of the number of peroxisomal proteins identified from different tissues by different studies.

**Supplemental Figure S6.** Heat maps showing relative expression levels of genes that encode peroxisomal proteins identified from etiolated seedlings in this study.

**Supplemental Figure S7.** Phenotypic analysis of the mutants of the newly validated peroxisomal genes.

**Supplemental Table S1.** Proteins identified from total peroxisomes in experiment T1.

**Supplemental Table S2.** Proteins identified from total peroxisomes in experiment T2.

**Supplemental Table S3.** Proteins identified from ZOOM 1 fraction pH 3.0 to 4.6.

**Supplemental Table S4.** Proteins identified from ZOOM 2 fraction pH 4.6 to 6.2.

**Supplemental Table S5.** Proteins identified from ZOOM 3 fraction pH 6.2 to 7.0.

**Supplemental Table S6.** Proteins identified from ZOOM 4 fraction pH 7.0 to 10.0.

**Supplemental Table S7.** Proteins identified from peroxisomal membrane proteomics.

**Supplemental Table S8.** Summary of nonredundant proteins identified from the seven proteomic experiments in this study.

**Supplemental Table S9.** Proteins tested for subcellular localization in this study.

**Supplemental Table S10.** Proteins identified from three plant peroxisome proteomic studies.

**Supplemental Table S11.** Proteins common or exclusive to the peroxisomal proteome of cell culture, leaves, or etiolated seedlings.

**Supplemental Table S12.** Data used to generate the heat maps in Figure 5A and Supplemental Figure S6A.

**Supplemental Table S13.** Details of the AtGenExpress data sets used in Supplemental Figure S6A.

**Supplemental Table S14.** Data used to generate the heat maps in Figure 5B and Supplemental Figure S6B.

**Supplemental Table S15.** Primers used for subcellular localization.

**Supplemental Table S16.** Primers used for genotyping and RT-PCR analysis.

**Supplemental Document S1.** MS/MS spectra for single peptide identifications.

**Supplemental Document S2.** Sequences used for the alignment shown in Figure 4.

## ACKNOWLEDGMENTS

We thank Doug Whitten of the Michigan State University proteomics facility for performing the LC-MS/MS analysis, the Arabidopsis Biological Resource Center and the Nottingham Arabidopsis Stock Centre for providing complementary DNA clones and seeds, Clint Chapple (Purdue University) for *bzo1* seeds, Bonnie Bartel (Rice University) for Arabidopsis PEX14 antibody, John Froehlich (Michigan State University) for pea Tic 110 antibody, and Rachel Capouya (University of Georgia) for technical assistance. We also thank the anonymous reviewers for their suggestions to improve our presentation of the proteomic data.

Received June 22, 2013; accepted October 15, 2013; published October 15, 2013.

## LITERATURE CITED

**Albrecht V, Simková K, Carrie C, Delannoy E, Giraud E, Whelan J, Small ID, Apel K, Badger MR, Pogson BJ** (2010) The cytoskeleton and the peroxisomal-targeted snowy cotyledon3 protein are required for chloroplast development in *Arabidopsis*. Plant Cell **22:** 3423–3438

**Arai Y, Hayashi M, Nishimura M** (2008a) Proteomic analysis of highly purified peroxisomes from etiolated soybean cotyledons. Plant Cell Physiol **49:** 526–539

**Arai Y, Hayashi M, Nishimura M** (2008b) Proteomic identification and characterization of a novel peroxisomal adenine nucleotide transporter supplying ATP for fatty acid beta-oxidation in soybean and *Arabidopsis*. Plant Cell **20:** 3227–3240

**Aung K, Hu J** (2011) The *Arabidopsis* tail-anchored protein PEROXISOMAL AND MITOCHONDRIAL DIVISION FACTOR1 is involved in the morphogenesis and proliferation of peroxisomes and mitochondria. Plant Cell **23:** 4446–4461

**Aung K, Hu J** (2012) Differential roles of Arabidopsis dynamin-related proteins DRP3A, DRP3B, and DRP5B in organelle division. J Integr Plant Biol **54:** 921–931

**Babujee L, Wurtz V, Ma C, Lueder F, Soni P, van Dorsselaer A, Reumann S** (2010) The proteome map of spinach leaf peroxisomes indicates partial compartmentalization of phylloquinone (vitamin K1) biosynthesis in plant peroxisomes. J Exp Bot **61:** 1441–1453

**Bednarek P, Pislewska-Bednarek M, Svatos A, Schneider B, Doubsky J, Mansurova M, Humphry M, Consonni C, Panstruga R, Sanchez-Vallet A, et al** (2009) A glucosinolate metabolism pathway in living plant cells mediates broad-spectrum antifungal defense. Science **323:** 101–106

**Beevers H** (1979) Microbodies in higher plants. Annu Rev Plant Physiol **30:** 159–193

**Beuerle T, Pichersky E** (2002) Enzymatic synthesis and purification of aromatic coenzyme A esters. Anal Biochem **302:** 305–312

**Breidenbach RW, Kahn A, Beevers H** (1968) Characterization of glyoxysomes from castor bean endosperm. Plant Physiol **43:** 705–713

**Brown PD, Tokuhisa JG, Reichelt M, Gershenzon J** (2003) Variation of glucosinolate accumulation among different organs and developmental stages of Arabidopsis thaliana. Phytochemistry **62:** 471–481

**Carrie C, Giraud E, Duncan O, Xu L, Wang Y, Huang S, Clifton R, Murcha M, Filipovska A, Rackham O, et al** (2010) Conserved and novel functions for Arabidopsis thaliana MIA40 in assembly of proteins in mitochondria and peroxisomes. J Biol Chem **285:** 36138–36148

**Carrie C, Giraud E, Whelan J** (2009a) Protein transport in organelles: dual targeting of proteins to mitochondria and chloroplasts. FEBS J **276:** 1187–1195

**Carrie C, Kühn K, Murcha MW, Duncan O, Small ID, O'Toole N, Whelan J** (2009b) Approaches to defining dual-targeted proteins in Arabidopsis. Plant J **57:** 1128–1139

**Carrie C, Murcha MW, Millar AH, Smith SM, Whelan J** (2007) Nine 3-ketoacyl-CoA thiolases (KATs) and acetoacetyl-CoA thiolases (ACATs) encoded by five genes in Arabidopsis thaliana are targeted either to peroxisomes or cytosol but not to mitochondria. Plant Mol Biol **63:** 97–108

**Clauss K, Baumert A, Nimtz M, Milkowski C, Strack D** (2008) Role of a GDSL lipase-like protein as sinapine esterase in Brassicaceae. Plant J **53:** 802–813

**Clay NK, Adio AM, Denoux C, Jander G, Ausubel FM** (2009) Glucosinolate metabolites required for an Arabidopsis innate immune response. Science **323:** 95–101

**Coca M, San Segundo B** (2010) AtCPK1 calcium-dependent protein kinase mediates pathogen resistance in Arabidopsis. Plant J **63:** 526–540

**Colquhoun TA, Marciniak DM, Wedde AE, Kim JY, Schwieterman ML, Levin LA, Van Moerkercke A, Schuurink RC, Clark DG** (2012) A peroxisomally localized acyl-activating enzyme is required for volatile benzenoid formation in a Petunia × hybrida cv. 'Mitchell Diploid' flower. J Exp Bot **63:** 4821–4833

**Cornah JE, Germain V, Ward JL, Beale MH, Smith SM** (2004) Lipid utilization, gluconeogenesis, and seedling growth in Arabidopsis mutants lacking the glyoxylate cycle enzyme malate synthase. J Biol Chem **279:** 42916–42923

**Cui S, Fukao Y, Mano S, Yamada K, Hayashi M, Nishimura M** (2013) Proteomic analysis reveals that the Rab GTPase RabE1c is involved in the degradation of the peroxisomal protein receptor PEX7 (peroxin 7). J Biol Chem **288:** 6014–6023

**Desai M, Hu J** (2008) Light induces peroxisome proliferation in Arabidopsis seedlings through the photoreceptor phytochrome A, the transcription factor HY5 HOMOLOG, and the peroxisomal protein PEROXIN11b. Plant Physiol **146:** 1117–1127

**Dixon GH, Kornberg HL** (1959) Assay methods for key enzymes of the glyoxylate cycle. Proc Biochem Soc **72:** 3P

**Eastmond PJ, Germain V, Lange PR, Bryce JH, Smith SM, Graham IA** (2000) Postgerminative growth and lipid catabolism in oilseeds lacking the glyoxylate cycle. Proc Natl Acad Sci USA **97:** 5669–5674

**Eubel H, Meyer EH, Taylor NL, Bussell JD, O'Toole N, Heazlewood JL, Castleden I, Small ID, Smith SM, Millar AH** (2008) Novel proteins, putative membrane transporters, and an integrated metabolic network are revealed by quantitative proteomic analysis of Arabidopsis cell culture peroxisomes. Plant Physiol **148:** 1809–1829

**Floerl S, Majcherczyk A, Possienke M, Feussner K, Tappe H, Gatz C, Feussner I, Kües U, Polle A** (2012) Verticillium longisporum infection affects the leaf apoplastic proteome, metabolome, and cell wall properties in Arabidopsis thaliana. PLoS ONE **7:** e31435

**Footitt S, Marquez J, Schmuths H, Baker A, Theodoulou FL, Holdsworth M** (2006) Analysis of the role of COMATOSE and peroxisomal beta-oxidation in the determination of germination potential in Arabidopsis. J Exp Bot **57:** 2805–2814

**Foyer CH, Bloom AJ, Queval G, Noctor G** (2009) Photorespiratory metabolism: genes, mutants, energetics, and redox signaling. Annu Rev Plant Biol **60:** 455–484

**Fraser CM, Rider LW, Chapple C** (2005) An expression and bioinformatics analysis of the Arabidopsis serine carboxypeptidase-like gene family. Plant Physiol **138:** 1136–1148

**Freitag J, Ast J, Bölker M** (2012) Cryptic peroxisomal targeting via alternative splicing and stop codon read-through in fungi. Nature **485:** 522–525

**Fukao Y, Hayashi M, Hara-Nishimura I, Nishimura M** (2003) Novel glyoxysomal protein kinase, GPK1, identified by proteomic analysis of glyoxysomes in etiolated cotyledons of Arabidopsis thaliana. Plant Cell Physiol **44:** 1002–1012

**Fukao Y, Hayashi M, Nishimura M** (2002) Proteomic analysis of leaf peroxisomal proteins in greening cotyledons of Arabidopsis thaliana. Plant Cell Physiol **43:** 689–696

**Gebhardt JS, Wadsworth GJ, Matthews BF** (1998) Characterization of a single soybean cDNA encoding cytosolic and glyoxysomal isozymes of aspartate aminotransferase. Plant Mol Biol **37:** 99–108

**Germain V, Rylott EL, Larson TR, Sherson SM, Bechtold N, Carde JP, Bryce JH, Graham IA, Smith SM** (2001) Requirement for 3-ketoacyl-CoA thiolase-2 in peroxisome development, fatty acid beta-oxidation and breakdown of triacylglycerol in lipid bodies of Arabidopsis seedlings. Plant J **28:** 1–12

**Gershater MC, Cummins I, Edwards R** (2007) Role of a carboxylesterase in herbicide bioactivation in Arabidopsis thaliana. J Biol Chem **282:** 21460–21466

**Goepfert S, Vidoudez C, Tellgren-Roth C, Delessert S, Hiltunen JK, Poirier Y** (2008) Peroxisomal delta(3), delta(2)-enoyl CoA isomerases and evolution of cytosolic paralogues in embrophytes. Plant J **56:** 728–742

**Gronemeyer T, Wiese S, Ofman R, Bunse C, Pawlas M, Hayen H, Eisenacher M, Stephan C, Meyer HE, Waterham HR, et al** (2013a) The proteome of human liver peroxisomes: identification of five new peroxisomal constituents by a label-free quantitative proteomics survey. PLoS ONE **8:** e57395

**Gronemeyer T, Wiese S, Grinhagens S, Schollenberger L, Satyagraha A, Huber LA, Meyer HE, Warscheid B, Just WW** (2013b) Localization of Rab proteins to peroxisomes: a proteomics and immunofluorescence study. FEBS Lett **587:** 328–338

**Guo L, Devaiah SP, Narasimhan R, Pan X, Zhang Y, Zhang W, Wang X** (2012) Cytosolic glyceraldehyde-3-phosphate dehydrogenases interact with phospholipase Dδ to transduce hydrogen peroxide signals in the *Arabidopsis* response to stress. Plant Cell **24:** 2200–2212

**Havelund JF, Thelen JJ, Møller IM** (2013) Biochemistry, proteomics, and phosphoproteomics of plant mitochondria from non-photosynthetic cells. Front Plant Sci **4:** 51

**Hayashi M, Nito K, Toriyama-Kato K, Kondo M, Yamaya T, Nishimura M** (2000) AtPex14p maintains peroxisomal functions by determining protein targeting to three kinds of plant peroxisomes. EMBO J **19:** 5701–5710

**Hayashi M, Toriyama K, Kondo M, Nishimura M** (1998) 2,4-Dichlorophenoxybutyric acid-resistant mutants of *Arabidopsis* have defects in glyoxysomal fatty acid beta-oxidation. Plant Cell **10:** 183–195

**Helm M, Lück C, Prestele J, Hierl G, Huesgen PF, Fröhlich T, Arnold GJ, Adamska I, Görg A, Lottspeich F, et al** (2007) Dual specificities of the glyoxysomal/peroxisomal processing protease Deg15 in higher plants. Proc Natl Acad Sci USA **104:** 11501–11506

**Hu J** (2009) Molecular basis of peroxisome division and proliferation in plants. Int Rev Cell Mol Biol **279:** 79–99

**Hu J, Baker A, Bartel B, Linka N, Mullen RT, Reumann S, Zolman BK** (2012) Plant peroxisomes: biogenesis and function. Plant Cell **24:** 2279–2303

**Hunter S, Jones P, Mitchell A, Apweiler R, Attwood TK, Bateman A, Bernard T, Binns D, Bork P, Burge S, et al** (2012) InterPro in 2011: new developments in the family and domain prediction database. Nucleic Acids Res **40:** D306–D312

**Ibdah M, Pichersky E** (2009) Arabidopsis Chy1 null mutants are deficient in benzoic acid-containing glucosinolates in the seeds. Plant Biol (Stuttg) **11:** 574–581

**Islinger M, Lüers GH, Li KW, Loos M, Völkl A** (2007) Rat liver peroxisomes after fibrate treatment: a survey using quantitative mass spectrometry. J Biol Chem **282:** 23055–23069

**Johnson MA, Snyder WB, Cereghino JL, Veenhuis M, Subramani S, Cregg JM** (2001) Pichia pastoris Pex14p, a phosphorylated peroxisomal membrane protein, is part of a PTS-receptor docking complex and interacts with many peroxins. Yeast **18:** 621–641

**Johnson TL, Olsen LJ** (2001) Building new models for peroxisome biogenesis. Plant Physiol **127:** 731–739

**Jones AM, MacLean D, Studholme DJ, Serna-Sanz A, Andreasson E, Rathjen JP, Peck SC** (2009) Phosphoproteomic analysis of nuclei-enriched fractions from Arabidopsis thaliana. J Proteomics **72:** 439–451

**Kanai M, Nishimura M, Hayashi M** (2010) A peroxisomal ABC transporter promotes seed germination by inducing pectin degradation under the control of ABI5. Plant J **62:** 936–947

**Kaschani F, Gu C, Niessen S, Hoover H, Cravatt BF, van der Hoorn RA** (2009) Diversity of serine hydrolase activities of unchallenged and

Botrytis-infected Arabidopsis thaliana. Mol Cell Proteomics **8:** 1082–1093

**Kataya AR, Reumann S** (2010) Arabidopsis glutathione reductase 1 is dually targeted to peroxisomes and the cytosol. Plant Signal Behav **5:** 171–175

**Kaur N, Hu J** (2011) Defining the plant peroxisomal proteome: from Arabidopsis to rice. Front Plant Sci **2:** 103

**Kaur N, Li J, Hu J** (2013) Peroxisomes and photomorphogenesis. Subcell Biochem **69:** 195–211

**Kaur N, Reumann S, Hu J** (2009) Peroxisome biogenesis and function. The Arabidopsis Book **7:** e0123 doi/0110.1199/tab.0123

**Keller A, Nesvizhskii AI, Kolker E, Aebersold R** (2002) Empirical statistical model to estimate the accuracy of peptide identifications made by MS/MS and database search. Anal Chem **74:** 5383–5392

**Kikuchi M, Hatano N, Yokota S, Shimozawa N, Imanaka T, Taniguchi H** (2004) Proteomic analysis of rat liver peroxisome: presence of peroxisome-specific isozyme of Lon protease. J Biol Chem **279:** 421–428

**Kleffmann T, von Zychlinski A, Russenberger D, Hirsch-Hoffmann M, Gehrig P, Gruissem W, Baginsky S** (2007) Proteome dynamics during plastid differentiation in rice. Plant Physiol **143:** 912–923

**Klempien A, Kaminaga Y, Qualley A, Nagegowda DA, Widhalm JR, Orlova I, Shasany AK, Taguchi G, Kish CM, Cooper BR, et al** (2012) Contribution of CoA ligases to benzenoid biosynthesis in petunia flowers. Plant Cell **24:** 2015–2030

**Kliebenstein DJ, D'Auria JC, Behere AS, Kim JH, Gunderson KL, Breen JN, Lee G, Gershenzon J, Last RL, Jander G** (2007) Characterization of seed-specific benzoyloxyglucosinolate mutations in Arabidopsis thaliana. Plant J **51:** 1062–1076

**Komori M, Kiel JA, Veenhuis M** (1999) The peroxisomal membrane protein Pex14p of Hansenula polymorpha is phosphorylated in vivo. FEBS Lett **457:** 397–399

**Lamberto I, Percudani R, Gatti R, Folli C, Petrucco S** (2010) Conserved alternative splicing of *Arabidopsis* transthyretin-like determines protein localization and *S*-allantoin synthesis in peroxisomes. Plant Cell **22:** 1564–1574

**Lanyon-Hogg T, Warriner SL, Baker A** (2010) Getting a camel through the eye of a needle: the import of folded proteins by peroxisomes. Biol Cell **102:** 245–263

**Lee CP, Taylor NL, Millar AH** (2013) Recent advances in the composition and heterogeneity of the Arabidopsis mitochondrial proteome. Front Plant Sci **4:** 4

**Lee S, Kaminaga Y, Cooper B, Pichersky E, Dudareva N, Chapple C** (2012) Benzoylation and sinapoylation of glucosinolate R-groups in Arabidopsis. Plant J **72:** 411–422

**Li J, Brader G, Helenius E, Kariola T, Palva ET** (2012) Biotin deficiency causes spontaneous cell death and activation of defense signaling. Plant J **70:** 315–326

**Lingard MJ, Bartel B** (2009) Arabidopsis LON2 is necessary for peroxisomal function and sustained matrix protein import. Plant Physiol **151:** 1354–1365

**Lingard MJ, Trelease RN** (2006) Five Arabidopsis peroxin 11 homologs individually promote peroxisome elongation, duplication or aggregation. J Cell Sci **119:** 1961–1972

**Lingner T, Kataya AR, Antonicelli GE, Benichou A, Nilssen K, Chen XY, Siemsen T, Morgenstern B, Meinicke P, Reumann S** (2011) Identification of novel plant peroxisomal targeting signals by a combination of machine learning methods and in vivo subcellular targeting analyses. Plant Cell **23:** 1556–1572

**Lipka V, Dittgen J, Bednarek P, Bhat R, Wiermer M, Stein M, Landtag J, Brandt W, Rosahl S, Scheel D, et al** (2005) Pre- and postinvasion defenses both contribute to nonhost resistance in Arabidopsis. Science **310:** 1180–1183

**Lowry OH, Rosebrough NJ, Farr AL, Randall RJ** (1951) Protein measurement with the folin phenol reagent. J Biol Chem **193:** 265–275

**Ma C, Haslbeck M, Babujee L, Jahn O, Reumann S** (2006) Identification and characterization of a stress-inducible and a constitutive small heat-shock protein targeted to the matrix of plant peroxisomes. Plant Physiol **141:** 47–60

**Mallory AC, Ely L, Smith TH, Marathe R, Anandalakshmi R, Fagard M, Vaucheret H, Pruss G, Bowman L, Vance VB** (2001) HC-Pro suppression of transgene silencing eliminates the small RNAs but not transgene methylation or the mobile signal. Plant Cell **13:** 571–583

**Mancuso DJ, Jenkins CM, Sims HF, Cohen JM, Yang J, Gross RW** (2004) Complex transcriptional and translational regulation of iPLAgamma resulting in multiple gene products containing dual competing sites for mitochondrial or peroxisomal localization. Eur J Biochem **271:** 4709–4724

**Missihoun TD, Schmitz J, Klug R, Kirch HH, Bartels D** (2011) Betaine aldehyde dehydrogenase genes from Arabidopsis with different subcellular localization affect stress responses. Planta **233:** 369–382

**Monroe-Augustus M, Ramón NM, Ratzel SE, Lingard MJ, Christensen SE, Murali C, Bartel B** (2011) Matrix proteins are inefficiently imported into Arabidopsis peroxisomes lacking the receptor-docking peroxin PEX14. Plant Mol Biol **77:** 1–15

**Muñoz-Bertomeu J, Cascales-Miñana B, Mulet JM, Baroja-Fernández E, Pozueta-Romero J, Kuhn JM, Segura J, Ros R** (2009) Plastidial glyceraldehyde-3-phosphate dehydrogenase deficiency leads to altered root development and affects the sugar and amino acid balance in Arabidopsis. Plant Physiol **151:** 541–558

**Nakagami H, Sugiyama N, Mochida K, Daudi A, Yoshida Y, Toyoda T, Tomita M, Ishihama Y, Shirasu K** (2010) Large-scale comparative phosphoproteomics identifies conserved phosphorylation sites in plants. Plant Physiol **153:** 1161–1174

**Narsai R, Law SR, Carrie C, Xu L, Whelan J** (2011) In-depth temporal transcriptome profiling reveals a crucial developmental switch with roles for RNA processing and organelle metabolism that are essential for germination in Arabidopsis. Plant Physiol **157:** 1342–1362

**Nesvizhskii AI, Keller A, Kolker E, Aebersold R** (2003) A statistical model for identifying proteins by tandem mass spectrometry. Anal Chem **75:** 4646–4658

**Nishimura M, Yamaguchi J, Mori H, Akazawa T, Yokota S** (1986) Immunocytochemical analysis shows that glyoxysomes are directly transformed to leaf peroxisomes during greening of pumpkin cotyledons. Plant Physiol **81:** 313–316

**Ofman R, Speijer D, Leen R, Wanders RJ** (2006) Proteomic analysis of mouse kidney peroxisomes: identification of RP2p as a peroxisomal nudix hydrolase with acyl-CoA diphosphatase activity. Biochem J **393:** 537–543

**Okinaka Y, Yang CH, Herman E, Kinney A, Keen NT** (2002) The P34 syringolide elicitor receptor interacts with a soybean photorespiration enzyme, NADH-dependent hydroxypyruvate reductase. Mol Plant Microbe Interact **15:** 1213–1218

**Orth T, Reumann S, Zhang X, Fan J, Wenzel D, Quan S, Hu J** (2007) The PEROXIN11 protein family controls peroxisome proliferation in *Arabidopsis*. Plant Cell **19:** 333–350

**Paoletti AC, Parmely TJ, Tomomori-Sato C, Sato S, Zhu D, Conaway RC, Conaway JW, Florens L, Washburn MP** (2006) Quantitative proteomic analysis of distinct mammalian Mediator complexes using normalized spectral abundance factors. Proc Natl Acad Sci USA **103:** 18928–18933

**Penfield S, Pinfield-Wells HM, Graham I** (2006) Storage reserve mobilisation and seedling establishment in Arabidopsis. The Arabidopsis Book **4:** e0100 doi/10.1199/tab.0100

**Peschke F, Kretsch T** (2011) Genome-wide analysis of light-dependent transcript accumulation patterns during early stages of Arabidopsis seedling deetiolation. Plant Physiol **155:** 1353–1366

**Peterhansel C, Horst I, Niessen M, Blume C, Kebeish R, Kurkcuoglu S, Kreuzaler F** (2010) Photorespiration. The Arabidopsis Book **8:** e0130 doi/10.1199/tab.0130

**Petersen BL, Chen S, Hansen CH, Olsen CE, Halkier BA** (2002) Composition and content of glucosinolates in developing Arabidopsis thaliana. Planta **214:** 562–571

**Pinfield-Wells H, Rylott EL, Gilday AD, Graham S, Job K, Larson TR, Graham IA** (2005) Sucrose rescues seedling establishment but not germination of Arabidopsis mutants disrupted in peroxisomal fatty acid catabolism. Plant J **43:** 861–872

**Pracharoenwattana I, Cornah JE, Smith SM** (2005) Arabidopsis peroxisomal citrate synthase is required for fatty acid respiration and seed germination. Plant Cell **17:** 2037–2048

**Pracharoenwattana I, Smith SM** (2008) When is a peroxisome not a peroxisome? Trends Plant Sci **13:** 522–525

**Qualley AV, Widhalm JR, Adebesin F, Kish CM, Dudareva N** (2012) Completion of the core $\beta$-oxidative pathway of benzoic acid biosynthesis in plants. Proc Natl Acad Sci USA **109:** 16383–16388

**Quan S, Switzenberg R, Reumann S, Hu J** (2010) In vivo subcellular targeting analysis validates a novel peroxisome targeting signal type 2 and

the peroxisomal localization of two proteins with putative functions in defense in Arabidopsis. Plant Signal Behav **5:** 151–153

**Reiland S, Finazzi G, Endler A, Willig A, Baerenfaller K, Grossmann J, Gerrits B, Rutishauser D, Gruissem W, Rochaix JD, et al** (2011) Comparative phosphoproteome profiling reveals a function of the STN8 kinase in fine-tuning of cyclic electron flow (CEF). Proc Natl Acad Sci USA **108:** 12955–12960

**Reiland S, Messerli G, Baerenfaller K, Gerrits B, Endler A, Grossmann J, Gruissem W, Baginsky S** (2009) Large-scale Arabidopsis phosphoproteome profiling reveals novel chloroplast kinase substrates and phosphorylation networks. Plant Physiol **150:** 889–903

**Reumann S** (2004) Specification of the peroxisome targeting signals type 1 and type 2 of plant peroxisomes by bioinformatics analyses. Plant Physiol **135:** 783–800

**Reumann S, Babujee L, Ma C, Wienkoop S, Siemsen T, Antonicelli GE, Rasche N, Lüder F, Weckwerth W, Jahn O** (2007) Proteome analysis of *Arabidopsis* leaf peroxisomes reveals novel targeting peptides, metabolic pathways, and defense mechanisms. Plant Cell **19:** 3170–3193

**Reumann S, Quan S, Aung K, Yang P, Manandhar-Shrestha K, Holbrook D, Linka N, Switzenberg R, Wilkerson CG, Weber AP, et al** (2009) In-depth proteome analysis of Arabidopsis leaf peroxisomes combined with in vivo subcellular targeting verification indicates novel metabolic and regulatory functions of peroxisomes. Plant Physiol **150:** 125–143

**Reumann S, Weber AP** (2006) Plant peroxisomes respire in the light: some gaps of the photorespiratory C2 cycle have become filled—others remain. Biochim Biophys Acta **1763:** 1496–1510

**Richau KH, Kaschani F, Verdoes M, Pansuriya TC, Niessen S, Stüber K, Colby T, Overkleeft HS, Bogyo M, Van der Hoorn RA** (2012) Subclassification and biochemical analysis of plant papain-like cysteine proteases displays subfamily-specific characteristics. Plant Physiol **158:** 1583–1599

**Rius SP, Casati P, Iglesias AA, Gomez-Casati DF** (2006) Characterization of an Arabidopsis thaliana mutant lacking a cytosolic non-phosphorylating glyceraldehyde-3-phosphate dehydrogenase. Plant Mol Biol **61:** 945–957

**Rojas CM, Senthil-Kumar M, Wang K, Ryu CM, Kaundal A, Mysore KS** (2012) Glycolate oxidase modulates reactive oxygen species-mediated signal transduction during nonhost resistance in *Nicotiana benthamiana* and *Arabidopsis*. Plant Cell **24:** 336–352

**Russell L, Larner V, Kurup S, Bougourd S, Holdsworth M** (2000) The Arabidopsis COMATOSE locus regulates germination potential. Development **127:** 3759–3767

**Sapir-Mir M, Mett A, Belausov E, Tal-Meshulam S, Frydman A, Gidoni D, Eyal Y** (2008) Peroxisomal localization of Arabidopsis isopentenyl diphosphate isomerases suggests that part of the plant isoprenoid mevalonic acid pathway is compartmentalized to peroxisomes. Plant Physiol **148:** 1219–1228

**Sautter C** (1986) Microbody transition in greening watermelon cotyledons: double immunocytochemical labeling of isocitrate lyase and hydroxypyruvate reductase. Planta **167:** 491–503

**Schilmiller AL, Koo AJ, Howe GA** (2007) Functional diversification of acyl-coenzyme A oxidases in jasmonic acid biosynthesis and action. Plant Physiol **143:** 812–824

**Schmid M, Davison TS, Henz SR, Pape UJ, Demar M, Vingron M, Schölkopf B, Weigel D, Lohmann JU** (2005) A gene expression map of Arabidopsis thaliana development. Nat Genet **37:** 501–506

**Schollenberger L, Gronemeyer T, Huber CM, Lay D, Wiese S, Meyer HE, Warscheid B, Saffrich R, Peränen J, Gorgas K, et al** (2010) RhoA regulates peroxisome association to microtubules and the actin cytoskeleton. PLoS ONE **5:** e13886

**Schrader M, Bonekamp NA, Islinger M** (2012) Fission and proliferation of peroxisomes. Biochim Biophys Acta **1822:** 1343–1357

**Schuhmann H, Huesgen PF, Gietl C, Adamska I** (2008) The DEG15 serine protease cleaves peroxisomal targeting signal 2-containing proteins in Arabidopsis. Plant Physiol **148:** 1847–1856

**Shindo T, Misas-Villamil JC, Hörger AC, Song J, van der Hoorn RA** (2012) A role in immunity for Arabidopsis cysteine protease RD21, the ortholog of the tomato immune protease C14. PLoS ONE **7:** e29317

**Shockey JM, Fulda MS, Browse J** (2003) Arabidopsis contains a large superfamily of acyl-activating enzymes: phylogenetic and biochemical analysis reveals a new class of acyl-coenzyme A synthetases. Plant Physiol **132:** 1065–1076

**Sirover MA** (2011) On the functional diversity of glyceraldehyde-3-phosphate dehydrogenase: biochemical mechanisms and regulatory control. Biochim Biophys Acta **1810:** 741–751

**Sugiyama N, Nakagami H, Mochida K, Daudi A, Tomita M, Shirasu K, Ishihama Y** (2008) Large-scale phosphorylation mapping reveals the extent of tyrosine phosphorylation in Arabidopsis. Mol Syst Biol **4:** 193

**Taler D, Galperin M, Benjamin I, Cohen Y, Kenigsbuch D** (2004) Plant *eR* genes that encode photorespiratory enzymes confer resistance against disease. Plant Cell **16:** 172–184

**Tanz SK, Castleden I, Hooper CM, Vacher M, Small I, Millar HA** (2013) SUBA3: a database for integrating experimentation and prediction to define the SUBcellular location of proteins in Arabidopsis. Nucleic Acids Res **41:** D1185–D1191

**Thabet I, Guirimand G, Courdavault V, Papon N, Godet S, Dutilleul C, Bouzid S, Giglioli-Guivarc'h N, Clastre M, Simkin AJ** (2011) The subcellular localization of periwinkle farnesyl diphosphate synthase provides insight into the role of peroxisome in isoprenoid biosynthesis. J Plant Physiol **168:** 2110–2116

**Thoms S, Debelyy MO, Nau K, Meyer HE, Erdmann R** (2008) Lpx1p is a peroxisomal lipase required for normal peroxisome morphology. FEBS J **275:** 504–514

**Tilton G, Shockey J, Browse J** (2000) Two families of acyl-CoA thioesterases in Arabidopsis. Biochem Soc Trans **28:** 946–947

**Titus DE, Becker WM** (1985) Investigation of the glyoxysome-peroxisome transition in germinating cucumber cotyledons using double-label immunoelectron microscopy. J Cell Biol **101:** 1288–1299

**Toufighi K, Brady SM, Austin R, Ly E, Provart NJ** (2005) The Botany Array Resource: e-northerns, expression angling, and promoter analyses. Plant J **43:** 153–163

**Tristan C, Shahani N, Sedlak TW, Sawa A** (2011) The diverse functions of GAPDH: views from different subcellular compartments. Cell Signal **23:** 317–323

**Tsuji A, Tsukamoto K, Iwamoto K, Ito Y, Yuasa K** (2013) Enzymatic characterization of germination-specific cysteine protease-1 expressed transiently in cotyledons during the early phase of germination. J Biochem **153:** 73–83

**van den Bosch H, Schutgens RB, Wanders RJ, Tager JM** (1992) Biochemistry of peroxisomes. Annu Rev Biochem **61:** 157–197

**Van Moerkercke A, Schauvinhold I, Pichersky E, Haring MA, Schuurink RC** (2009) A plant thiolase involved in benzoic acid biosynthesis and volatile benzenoid production. Plant J **60:** 292–302

**van Wijk KJ, Baginsky S** (2011) Plastid proteomics in higher plants: current state and future goals. Plant Physiol **155:** 1578–1588

**Vescovi M, Zaffagnini M, Festa M, Trost P, Lo Schiavo F, Costa A** (2013) Nuclear accumulation of cytosolic glyceraldehyde-3-phosphate dehydrogenase in cadmium-stressed Arabidopsis roots. Plant Physiol **162:** 333–346

**Vlot AC, Liu PP, Cameron RK, Park SW, Yang Y, Kumar D, Zhou F, Padukkavidana T, Gustafsson C, Pichersky E, et al** (2008) Identification of likely orthologs of tobacco salicylic acid-binding protein 2 and their role in systemic acquired resistance in Arabidopsis thaliana. Plant J **56:** 445–456

**von Zychlinski A, Kleffmann T, Krishnamurthy N, Sjölander K, Baginsky S, Gruissem W** (2005) Proteome analysis of the rice etioplast: metabolic and regulatory networks and novel protein functions. Mol Cell Proteomics **4:** 1072–1084

**Wang X, Bian Y, Cheng K, Gu LF, Ye M, Zou H, Sun SS, He JX** (2013) A large-scale protein phosphorylation analysis reveals novel phosphorylation motifs and phosphoregulatory networks in Arabidopsis. J Proteomics **78:** 486–498

**Weitbrecht K, Müller K, Leubner-Metzger G** (2011) First off the mark: early seed germination. J Exp Bot **62:** 3289–3309

**Widhalm JR, Ducluzeau AL, Buller NE, Elowsky CG, Olsen LJ, Basset GJ** (2012) Phylloquinone (vitamin K(1)) biosynthesis in plants: two peroxisomal thioesterases of Lactobacillales origin hydrolyze 1,4-dihydroxy-2-naphthoyl-CoA. Plant J **71:** 205–215

**Wildermuth MC** (2006) Variations on a theme: synthesis and modification of plant benzoic acids. Curr Opin Plant Biol **9:** 288–296

**Yang J, Han X, Gross RW** (2003) Identification of hepatic peroxisomal phospholipase A(2) and characterization of arachidonic acid-containing choline glycerophospholipids in hepatic peroxisomes. FEBS Lett **546:** 247–250

**Zolman BK, Silva ID, Bartel B** (2001) The Arabidopsis *pxa1* mutant is defective in an ATP-binding cassette transporter-like protein required for peroxisomal fatty acid $\beta$-oxidation. Plant Physiol **127:** 1266–1278

**Zolman BK, Yoder A, Bartel B** (2000) Genetic analysis of indole-3-butyric acid responses in *Arabidopsis thaliana* reveals four mutant classes. Genetics **156:** 1323–1337